Prog. Oceanog. Vol. 33, pp.1-92, 1994.
Printed in Great Britain.

0079 - 6611/94 $24.00

On the total geostrophic circulation of the North Atlantic Ocean: Flow patterns, tracers, and transports

JOSEPH L. REID

Marine Life Research Group, Scripps Institution of Oceanography, 9500 Gilman Dr., La Jolla, California 92093-0230, U.S.A.

Abstract — This is an attempt to provide patterns of flow at all depths in the North Atlantic Ocean that balance the transport and are consistent with the patterns of characteristics. It identifies the paths of flow and the sources of the characteristics. In particular it attempts to account for the high heat and salt content of the deep North Atlantic in terms of an increment of very warm and saline Mediterranean water that partly circulates within the anticyclonic gyre of the North Atlantic and the cyclonic gyre to the south and east before passing southward into the South Atlantic. The direct effect of the Mediterranean outflow is to provide heat and salt to these gyres. The deeper water of these gyres has entered from the South Atlantic at depths below 1500 m and is colder and less saline than the waters to the north. The increment of heat and salt that pours into these waters as they pass northward along the eastern boundary is carried both northward to Iceland and westward across the Atlantic. Part of the northward flow carries higher salinities to mix with Norwegian Sea waters and become denser, though still relatively warm and saline. The westward component provides the high heat and salt content of the deep Gulf Stream and of the southward flow along the western boundary.

As a result the $0.7 \times 10^6 m^3 s^{-1}$ of very warm and saline water from the Mediterranean Sea is not immediately carried southward out of the North Atlantic but only after some excursions through these gyres. The residence time of the increments in the North Atlantic is therefore longer, and leads to an accumulation of heat and salt.

CONTENTS

1. INTRODUCTION

The purpose of this study is to estimate the general circulation of the North Atlantic Ocean in a manner that defines the flow at all depths and balances the geostrophic transport. The estimation is made through a new examination of the characteristics and the geostrophic shear. This method was used in a study of the South Atlantic (REID, 1989). Some of the maps prepared in that study and a few new maps are added to those prepared here for the North Atlantic so that the entire Atlantic Ocean is shown. The major difference from the results of earlier studies is the attempt to show that it is the contribution of the Mediterranean outflow that imposes upon the incoming circumpolar waters the distinctive characteristics that mark them as they return southward from the North Atlantic and extend into the deeper waters of the world ocean.

The two major assumptions used herein are that the flow is geostrophic and that both flow and mixing take place approximately along isopycnal surfaces. Characteristics acquired where the isopycnals outcrop, either in the open Atlantic or in the adjacent seas, are modified along the flow by both lateral and vertical diffusion. Some tracers show both lateral and vertical extrema in concentration and their patterns can be used to estimate the sense of flow.

The baroclinic flow is given by the density field, that is, the geostrophic flow relative to the bottom flow, which is estimated from examination of the various characteristics and taken as the reference velocity. The density field is defined fairly well over most of the North Atlantic Ocean by the present data set. While the flow is known to vary with time, the large-scale flow below the upper layer appears to be steady enough to allow data sets from different periods to be combined and the general circulation to be examined usefully.

The characteristics used as tracers have various sources and lie in various ranges of depth and density, and are spread throughout the ocean by both flow and mixing. Their patterns are examined along vertical sections and along isopycnal surfaces. In some density ranges the patterns are sharply defined and show features that appear to be the result of advection. For example, along the western boundary the characteristics indicate that the deepest waters derive from the south and the mid-depth waters from the north, and both appear to extend meridionally as features narrow enough to suggest advection rather than horizontal diffusion alone. These and other patterns, both shallower and deeper, can in some places indicate flow components at different depths that are in opposite senses, and with the measured baroclinic component, constrain the value of the reference velocity to a narrow range.

The area studied is shown in Fig. 1 on a Mollweide projection, with the pertinent topographic features labeled. Depths less than 3500 m are shaded and the 5000m contour is shown. The array of stations used in determining the fields of adjusted steric height and volume transport (Fig. 2) is selected to include stations that reached near the bottom and, where it is possible, long lines made by a single ship roughly normal to major flows. Some combinations of stations from different expeditions are needed to complete a few lines. For the North Atlantic 1102 stations are selected for calculating the fields of flow, and they are identified in Table 1. A much larger set of stations (2273) is used on the isopycnal maps.

The work was carried out in two stages. First, on selected lines of stations (Fig.2), components of geostrophic motion are calculated relative to the deepest common depth of each consecutive station pair. Where the sense of this baroclinic flow seems to be consonant with the tracer patterns, no reference velocity (at the bottom) is added initially. Where it seems not to be consonant with the sense indicated by the tracers, a reference velocity is added to achieve the sense assumed for that pair of stations. The adjusted flows normal to the station pairs along these lines define adjusted pressure gradients along the lines, and these are integrated horizontally to obtain the adjusted steric height. For each line the integration begins at the station pair nearest the coast and the value of steric height at the first station (usually in shallow water) varies from line to line. At the intersections the adjusted steric heights may not match. Some changes in the constants of integration for some lines and in the reference velocities between various station pairs can bring them into agreement.

A second stage is necessary because no constraint of continuity is used in the first stage, and the resulting transport may not be in balance. The transport into the South Atlantic Ocean through the Drake Passage is taken to be $130 \times 10^6 m^3 s^{-1}$ (WHITWORTH, NOWLIN, and WORLEY, 1982), and a net transport of $2 \times 10^6 m^3 s^{-1}$ into the North Atlantic from the Pacific through the Arctic Ocean is assumed. The transport of the Florida Current is taken to be $30 \times 10^6 m^3 s^{-1}$ and the flow into the Caribbean Sea partitioned about the same as ROEMMICH (1981) estimated. The net flow out of the Atlantic is $132 \times 10^6 m^3 s^{-1}$, the sum of the $130 \times 10^6 m^3 s^{-1}$ through the Drake Passage and the $2 \times 10^6 m^3 s^{-1}$ through the Arctic. A further adjustment to match these constraints required very little change in the reference velocities and resulting flow patterns. The reference velocities estimated between each station pair along the integration paths are shown in Fig. 3 for bottom depths of 1500 m and greater.

Except for the specified net transports through the Drake Passage, southward between the continents, and south of Africa, the only constraint applied herein is quite simple: that the large-scale flow should be qualitatively coherent with the tracer patterns. No constraint on heat or salt transport is applied and no Ekman transport accommodated.

2. LIMITATIONS

The method used here is of course quite subjective. Aside from this there are several other limitations, that may be less obvious. Not all of the measurements extended as close to the bottom as I would have liked. Station spacing across ridges and near the continental slopes is not always adequate. There are very few deep stations in the equatorial zone, and some, particularly the oxygen and nutrient data, are not of high quality.

While a coherent picture of a large-scale general circulation is presented here, there can be some question as to what it is meant to represent. The data are not synoptic nor are they the averages of measurements taken over a long period. The greatest differences in data where lines intersect are encountered in the upper few hundred meters and appear to result from seasonal and mesoscale variations. The irregular feature seen on Fig 8a — the 3.4 isopleth near 24°N, 60°W — is a consequence of the different times at which the lines of stations were made. Such differences occur at various intersections of the lines shown in Fig. 2 and result in a few extrema in the fields of adjusted steric height from the sea surface down to about 1000 decibars. At greater depths this effect is not severe, but several deep eddies are found.

The horizontal flow proposed here is illustrated in a set of maps of adjusted steric height along various isobaric surfaces from the sea surface to 5200 decibars. This study of steric height requires stations that extend to or near the bottom. As there are few such stations and lines taken near the equator, and the flow there is so highly variable as to require a nearly synoptic coverage, the area between about 8°N and 8°S is not well defined herein.

With the assumption that the large-scale pattern of subsurface flow does not vary too widely, I hope that the flow pictured here approximates the large-scale flow pattern that has obtained with only minor variations over some long period, perhaps as long as the 60 years over which the data were collected. The general circulation proposed here is of course not a unique solution for the tracer patterns: various parts of the opposing flows can be strengthened or weakened somewhat while still maintaining the balance of net transport and qualitative coherence with the tracer patterns. I believe, however, that the large-scale flow derived here is close enough to reality to be useful.

3. THE DATA PRESENTATION

All of the illustrations have been placed after the text. As some of them will be referred to in different sections of the text it seems easier to have them grouped in order of surface maps, vertical sections, maps of geostrophic flow, and maps of characteristics along isopycnals. The reader may wish to look at the figures before reading the sections that follow.

It must be kept in mind that the isopycnal surfaces mapped are not truly isentropic or ideal neutral surfaces. However, the ranges of the temperature and salinity fields are such that if chosen carefully these surfaces can be useful approximations of such idealized surfaces. The isopycnal surfaces are defined by different values at different pressures. As pointed out by REID and LYNN (1971), a deep parcel near the equator, defined by the density it would have at 4000 decibars, may extend to shallower depths and lower pressures both north and south of the equator. Where it rises in the Atlantic it will extend into warmer and more saline waters in the north, and into colder, fresher waters in the south; the potential density where it crosses 3000 decibars may be different at the northern and southern crossings. Following such surfaces from one pressure range to another in different areas requires different labels. Table 2 lists for each isopycnal mapped the σ-values in all its pressure ranges. It includes the values for the northern and southern extensions if they are different. Each isopycnal map is labeled with a single density-number, usually corresponding to the pressure-range of its greatest σ-value, and these values are bold-face in the table.

The International Equation of State for Seawater, 1980, as given by FOFONOFF (1985), is used herein and was used for the South Atlantic study (REID, 1989). The differences from the earlier Knudsen-Ekman version used for the South Pacific study (REID, 1986) are not significant to these results. The major difference is that the calculated density parameter will be lower in the new equation. That is, a value of 46.046 in σ_4 (near 4000 decibars) in the old equation corresponds to about 46.00 in the new equation.

4. THE EARLY WORK

The first attempts to examine the deeper circulation of the entire Atlantic Ocean were WÜST's (1935) study of the waters at and beneath the Intermediate Water and DEFANT's (1941a, 1941b) studies of the geostrophic circulation of the upper 2000 m. These were based upon data collected by the Meteor expedition of 1925-1927 in the South and Equatorial Atlantic and the accumulation of data collected by various other expeditions.

Wüst may have considered mapping the available tracers — salinity, temperature, and oxygen — along isopycnal surfaces. However, his study (1933) of potential density (referred to sea-surface pressure) found a maximum value above the bottom. This seemed to indicate an unstable water column. In a comment upon the study EKMAN (1934) resolved the apparent discrepancy, but Wüst was by this time committed to the method of cores — vertical extrema in the tracers — in his study of the circulation, which he published in 1935.

The cores he discussed were the salinity minimum from the south, which he called the Subantarctic Intermediate Water, the thick layer of saline water from the north which he divided into three layers, and the densest layer, from the south, which he called Antarctic Bottom Water.

He defined the shallowest of the three layers from the north by the maximum in salinity (Fig. 5b), which he called the upper North Atlantic Deep Water and accounted for by the outflow from the Mediterranean Sea, which extends westward across the Atlantic toward Cape Hatteras, turning southward along the western boundary and continuing into the South Atlantic. Beneath this flow he defined his Middle and Lower North Atlantic Deep Water by vertical maxima in oxygen, also extending southward along the western boundary from the Labrador and Irminger basins as far as 40°S. The oxygen minimum that separates the two deeper layers was not found consistently and the lower layer was not made clear enough to be mapped (Fig. 5d).

Overflow of dense water from the Norwegian-Greenland Sea (Fig. 5c) was not recognized at that time, and the general belief was that the deeper part of the southward-flowing water in the North Atlantic was formed by convection in the Irminger Sea.

The Gulf Stream recirculation was first shown by DEFANT (1941a,b) on his maps of both relative geostrophic flow and adjusted flow. It is an inescapable result of any plausible treatment of the geostrophic shear. A deep reference velocity to eliminate it would require an unrealistically high eastward flow south of the Gulf Stream at depths of 3000 m. Having seen Wüst's representation of the deep southward flow along the western boundary, Defant chose to place a shallow surface of zero flow along the western boundary in the North Atlantic. Except for the zone between about 20°N and 30°N, where the southward flow is weakest and the data available to him were both sparse and erratic, his formulation (1941b) portrays the deep western boundary undercurrent in both the North and South Atlantic in much the same form as it is recognized today.

Defant accepted Wüst's finding of the western boundary undercurrent (based on oxygen) but did not accept his westward flow of the Mediterranean tongue. If he had, and the data had been adequate, he would certainly have recognized that the return flow carried Mediterranean water.

5. THE NEAR-SURFACE WATERS: CHARACTERISTICS AND FLOW

The surface and near-surface maps (Fig. 4) are meant to show the general patterns of characteristics in the upper waters and especially the characteristics of the water at or near the outcrops of the isopycnals. It would be better to use data from the winter period of maximum convection and density, but this was not possible everywhere. For temperature, salinity, density, and oxygen it was necessary to include data from the period from November through April. Maps of the nutrients at the surface of the North Atlantic would show such low values nearly everywhere as to give little detail. Instead the nutrients have been mapped at a depth of 100 m. As there are few high-latitude nutrient data in winter, data from all seasons have been used.

The maps of temperature and salinity at the surface from these data (Figs. 4a-b) are not significantly different from other versions. The highest density of the surface layer of the open Atlantic is about 27.78 in σ_0, found just offshore of Greenland in the Labrador and Irminger basins, along the axis of the cyclonic gyre (Fig. 4c). This is the limiting outcrop of the open North Atlantic. Water of this density is not found deeper than about 1800 to 1900 m in the North Atlantic (just south of the Gulf Stream) and about 2000 m in the South Atlantic (along 40°S) (Fig. 13a). Values of 28.0 in σ_0 are found only in the Norwegian-Greenland Sea, and do not extend past the Iceland-Scotland sill.

The pattern of oxygen at the sea surface (Fig. 4d) is dominated by the temperature field, as might be expected. On the maps of nutrients at 100m depth (Figs. 4e-g) the highest values north of 50°S are found along 10°N and 10°S in the east, with a secondary high south of Greenland, in the area of highest density. The lowest values are found within the anticyclonic gyres, roughly in the regions of Ekman convergence, and the high values in the regions of divergence shown by HELLERMAN and ROSENSTEIN (1983).

Larger-scale studies of the North Atlantic Ocean have found an anticyclonic circulation in mid-latitudes, and this pattern of flow is seen on the map of adjusted steric height at the sea surface (Fig. 8a), which also shows the surface flow in the South Atlantic. A western boundary current emerges from the Florida Strait, continues northward as the Gulf Stream as far as Cape Hatteras and turns offshore to the east. Part of it turns back immediately and rejoins the Gulf Stream farther south. Another part continues eastward as the North Atlantic Current, turning both northward and southward in mid-ocean, with some part rejoining the Florida Current by way of the Caribbean Sea.

The eastward limb of the subarctic gyre includes the part of the North Atlantic Current that turns northward near 50°N as it nears the eastern boundary. Some of it enters the Norwegian Sea east of Iceland and some turns westward south of Iceland into the Irminger Sea. From there a part passes northward through the Denmark strait and part joins the East Greenland Current. This part passes southward and around the tip of Greenland to become the West Greenland Current, and then turns cyclonically to become the Labrador Current, which flows southward and divides near Newfoundland. Part of the Labrador Current turns eastward to rejoin the North Atlantic Current and part continues southwestward along the western boundary past 40°N and then turns back to the northeast with the Gulf Stream-North Atlantic Current, as discussed by IVERS (1975) and TSUCHIYA, TALLEY, and McCARTNEY (1992).

South of the anticyclonic gyre there is a northward flow across the equator along the western boundary and into the Caribbean Sea, and a counter-current flowing eastward along about 5° to 10°N (SCHMITZ and RICHARDSON, 1991). The flow field in the Caribbean Sea was based upon the same data used by ROEMMICH (1981), and in the Gulf of Mexico the same data used by HOFFMAN and WORLEY (1986). While the method of analysis used here was quite different the resultant fields of flow are similar.

The flow close to the equator cannot be represented in detail by the methods used here. The horizontal pressure gradients required to balance the flow become very weak, and transient disturbances and seasonal variations (ARNAULT, MORLIERE, MERLE, and MENARD, 1992) dominate the pattern. The vertical shears in the upper levels of stronger flow from more nearly synoptic data can provide a meaningful pattern almost to the equator (MERLE, 1978; RICHARDSON and McKEE, 1984; TSUCHIYA, 1985 and 1986). However, the data used herein are sparse and are from different periods. They extend to the bottom and hence are subject to different transients at different depths, and the flow field near the equator is not resolved well by these maps of steric height. Near the equator the tracers give much better information about the flow than does the density field.

There is a rough symmetry about the equator. The North and South Atlantic each have a mid-latitude anticyclonic gyre with a broad westward return flow, a high-latitude cyclonic gyre with a narrow equatorward extension along the western boundary, and eastward flows just north and south of the equator. The most significant differences are the northward flow across the equator in the west, and the eastward flow in the far South Atlantic, that feeds not only the Weddell Sea cyclonic gyre but extends as a gyre all around Antarctica.

6. THE DEEPER CIRCULATION

There are three deep gyral patterns in the North Atlantic, a deep southward flow along the western boundary and some zonal flows south of 10°N (Figs. 8a-n). Two of the gyres are the great mid-latitude anticyclonic gyre and the cyclonic gyre in the north. The third is a cyclonic gyre that is seen clearly only beneath the surface. It lies east and south of the anticyclonic gyre. All of these extend to great depths, but there are some additional features in the deeper waters. Some of these changes begin just below the sea surface (250 m to 500 m) and others at greater depths where the various ridges limit or guide the flow.

At the sea surface the anticyclonic gyre extends through about 40° of latitude in mid-ocean, but below 1000m it contracts northward. The eastward flow — the Gulf Stream-North Atlantic Current — follows about the same path as the surface flow down to the depth of the Mid-Atlantic Ridge, but the westward-returning limb lies farther north at greater depths and the breadth of the gyre is reduced to about 25° of latitude.

The flow of the northern cyclonic gyre is eastward near 50°N and turns northward near the eastern boundary, but below a few hundred meters part of it first loops southward near 20°W toward the Iberian Peninsula and then northward along the eastern boundary (HUTHNANCE and GOULD, 1989). In the north the westward-flowing limb of the cyclonic gyre is forced at greater depths to follow a sinuous path along the topography. It loops into and out of the Rockall Trough and the Iceland, Irminger and Labrador basins before dividing near the Grand Banks to flow both southwestward along the boundary and eastward across the Atlantic. The cyclonic gyre extends down to Ridge depth, but below about 1200 m some of its southward extension in the west does not turn back to the north near Cape Hatteras. Instead it continues along the western boundary and across the equator.

The third of the three large gyres of the North Atlantic is the cyclonic flow seen below the surface south and east of the anticyclonic gyre (REID, 1991). It consists of part of the westward limb of the anticyclonic gyre, the eastward flow near 10°N-20°N, and the poleward flow along the coast of Africa and Europe (SWALLOW, GOULD, and SAUNDERS, 1979; REID, 1979; SAUNDERS, 1982; BARTON, 1989). Its cyclonic flow pattern may correspond to the cyclonic gyre just south of the equator (Figs. 8a-8f). It is this gyre that at depths below 800 m (Figs. 8d-h) conducts the circumpolar water from south of the equator northward along the eastern boundary. Some of it continues northward to join the subarctic gyre and some turns back westward with the western limb of the great anticyclonic gyre, carrying the added heat and salt from the Mediterranean outflow westward across the Atlantic.

Below the crest of the Mid-Atlantic Ridge and down to about 4500 m (Figs. 8i-l) this cyclonic gyre appears to cover the entire eastern basin north of about 15°N. It is similar to the deep cyclonic pattern suggested by REID (1981), LONSDALE (1982) and DICKSON, GOULD, MÜLLER, and MAILLARD (1985). The extension of the deep flow into the northern cyclonic gyre has been shown by IVERS (1975), REID (1979), SAUNDERS (1987) and McCARTNEY (1992).

The deep southward flow that WÜST (1935) found along the western boundary from the Labrador and Irminger seas to the South Atlantic is seen clearly on the maps of flow. At depths above about 1000 m to 1200 m (Fig. 8e) the southward flow extends only to Cape Hatteras before turning back northeastward with the Gulf Stream. At greater depths (Fig. 8f) part of it continues southward all along the western boundary to about 40°S, where it shifts offshore of the northward flow from the far south. The maps of geostrophic flow can show the part of this deep flow that extends eastward along the equator, but they cannot show the cross-equatorial flow in the west. The southward flow along the western boundary is weakest near Cape Hatteras. Much of the flow from the far north turns back with the Gulf Stream north of 32°N, and the westward contribution to the southward flow takes place south of there.

The deep Gulf Stream begins north of 30°N where part of the westward limb of the anticyclonic gyre turns northward and is joined north of about 32°N by waters of the deep southward flow returning northward (Fig. 8f). There is no deep Gulf Stream south of about 30°N, but only the shallow Florida Current, which crosses the deeper southward flow just south of Cape Hatteras, and joins the anticyclonic gyre. This circulation has been discussed by RICHARDSON (1977) and by PICKART and SMETHIE (in press).

The other deep flows are the westward flow seen between about 5° and 10°N and the eastward flow along or near the equator at depths from about 800 m to the crest of the Mid-Atlantic Ridge (WÜST, 1935; WÜST and DEFANT, 1936). The westward flow may start from water that has crossed the equator in the east. The eastward flow along the equator carries some of the northern water from the southward flow along the western boundary. (The flow just south of the equator cannot be defined clearly by the available density data, but the characteristic patterns presented later suggest an eastward flow that splits northward and southward in the east.)

The map of deep currents prepared by McCAVE and TUCHOLKE (1986) is seen with the bottom velocities estimated here at depths greater than 2000 m (Fig. 8o). They are both based upon interpretation of observed characteristics. McCAVE and TUCHOLKE used the patterns in the sediments left by the flow, and I used the patterns of characteristics at all depths. There is a remarkable resemblance between the two results.

7. THE GEOSTROPHIC TRANSPORT

As the velocity field has been defined at all depths it can be integrated to produce a field of total geostrophic transport (Fig. 9) or the transport in selected depth or density ranges. No assumptions about the nature of transport were made initially other than those about the entering and departing quantities. The field of transport, then, is the result of the various velocities that were obtained by combining the baroclinic components with the bottom velocity derived from the tracer patterns along the isopycnals. There has been no attempt to match any earlier concept of the shape or magnitude of the flow field.

The integration starts from a zero value at the coast of Antarctica and reaches $130 \times 10^6 m^3 s^{-1}$ everywhere along the coasts of the American continents and Greenland. Along the coasts of Europe and Africa it reaches $132 \times 10^6 m^3 s^{-1}$, as $2 \times 10^6 m^3 s^{-1}$ are assumed entering through the Norwegian-Greenland Sea. South of the equator the field is taken from the earlier study (REID, 1989).

Aside from the Caribbean and Gulf of Mexico, which have no counterparts in the South Atlantic, there is some correspondence between the transports north and south of the equator. Note that because of the origin of the integration the gyres with high numbers in the centers are anticyclonic south of the equator and cyclonic in the north. Each ocean has an anticyclonic gyre in the west with a cyclonic turn near 10° to 20° latitude and a poleward flow along the eastern boundary, and a cyclonic gyre poleward of about 50° latitude. The major shift in the westward limb of the anticyclonic gyre takes place above 800 decibars, and except along the western boundary the flow direction in the North Atlantic is nearly uniform from there down to the crest of the Mid-Atlantic Ridge. The flow patterns in that range all resemble the pattern of total geostrophic transport. This does not mean that the flow is entirely barotropic. Their patterns are also (except of course for the southward flow along the western boundary) much like the baroclinic flow along 2000 decibars relative to 3500 decibars, shown by REID (1981).

A net southward transport along the western boundary is seen everywhere except between Cape Hatteras and about 26°N. It is here that the southward component is weakest, and where the Gulf Stream, with no deep component here, passes over it. This is much as suggested by WÜST (1935) and as can be seen in the maps by DEFANT (1941b). PICKART and SMETHIE (in press) have confirmed this pattern near Cape Hatteras using tracers and float data.

Within the Labrador Basin the cyclonic flow takes place from top to bottom around the northern and western boundaries. A great part of the upper layer turns offshore before reaching Cape Hatteras. To deal with the part of the deep southward flow that is continuous along the western boundary I have chosen the isopycnal where $\sigma_{1.5} = 34.64$ as a cap for it (Table 2 shows the corresponding σ values at lower pressures, with 27.777 in σ_0 in the upper layer). This isopycnal outcrops near the tip of Greenland but lies near 1000 m to 1200 m over most of the Labrador Basin, near 1400 m to 1600 m along the western boundary north of the equator, and from 1600 m to 2000 m in the South Atlantic, and outcrops south of 60°S (Fig. 13a). The flow along this isopycnal is shown on Fig. 13b. As the field of adjusted steric height has

been determined, the flow along an isopycnal can be obtained by lateral integration of the increments of steric height at the average depth of the isopycnal between each station pair.

Below this cap these results show a westward flow of 29 x $10^6 m^3 s^{-1}$ south of the tip of Greenland. CLARKE's (1984) results as cited in DICKSON, GMITROWICZ, and WATSON (1990), give only 13.3 x $10^6 m^3 s^{-1}$ there at densities greater than 27.8 in σ_0. McCARTNEY (1992) used that value in his calculation. Across the 59°N and 53°N sections the southward flow along the boundary is 27 x $10^6 m^3 s^{-1}$, decreasing to 23 across the 47°N section as some of the flow has turned eastward. Across 53°W the flow (now westward) along the boundary is 20 x $10^6 m^3 s^{-1}$ and across 58°W it rises slightly to 24 in a local intensification of both the westward and eastward flows. Across 64°W it is 11 and across 36°N it is 13. The minimum value is 7 x $10^6 m^3 s^{-1}$ across the 32°N section, just south of Cape Hatteras. This is the same value that SWALLOW and WORTHINGTON (1961) had found near there. The flow beneath the cap is 31 x $10^6 m^3 s^{-1}$ across 24°N, 30 across 16°N, 23 across 13°N, and 21 across 8°N.

The loss to the eastward flow along the equator cannot be estimated by this method, but the deep southward flow across 8°S near the western boundary is only 13 x $10^6 m^3 s^{-1}$. As it is joined by waters from the anticyclonic gyre of the South Atlantic it rises to 22 across 11°S and to 38 across 16°S (Figs. 8g-8j). As the gyre appears to be distorted by the Rio Grande Rise near 30°S — perhaps TSUCHIYA's (1985) double gyre offset at greater depth? — some of it turns back. The transport is 22 x $10^6 m^3 s^{-1}$ across 24°S and only 11 across the line extending southeastward from about 24°S at the coast to 32°S at 30°W. The gyre intensifies south of the Rise and the southward flow across 42°S is 36 x $10^6 m^3 s^{-1}$ as the deep western boundary current finally turns offshore.

Some of the southward transports given above are very much like those based upon different methods. The value of 31 x $10^6 m^3 s^{-1}$ is nearly the same as the 32 to 33 x $10^6 m^3 s^{-1}$ obtained near 26°N by LEE, JOHNS, SCHOTT, and ZANTOPP (1990) and LEAMAN and HARRIS (1990). MOLINARI, FINE, and JOHNS (1992), using tracers and density, estimated a southward transport of 26 x $10^6 m^3 s^{-1}$ in the flow near 4°N to 8°N. Their reference surface for velocity calculations was 4.7°C in potential temperature. This is somewhat shallower than the 34.64 in $\sigma_{1.5}$ that caps the deep southward flow here, and which resulted in 21 x $10^6 m^3 s^{-1}$ across 8°N.

HOGG (1983 and 1992), using direct current measurements near the western boundary, has suggested that between about 50°W and 65°W there is a tight cyclonic gyre between the Gulf Stream and the westward flow along the boundary, raising the transport of the Gulf Stream to 150 x $10^6 m^3 s^{-1}$ between 60°W and 55°W. My results do not show such a large increase. The closed cyclonic gyre appears clearly on the maps at 1500, 4500, and 5000 db (Figs. 8f, 8l and 8m) and along the bottom (Fig. 3). Locally, between 50°W and 60°W, it adds about 10 x $10^6 m^3 s^{-1}$ to both currents. The Gulf Stream transport rises to about 100 x $10^6 m^3 s^{-1}$ and the southwestward flow to about 35 x $10^6 m^3 s^{-1}$, and the larger values are restricted to about 50°W to 60°W.

Recent studies of the deep southward flow between about 18°N and the equator have found transports in the range from 20 to 26 x $10^6 m^3 s^{-1}$ (JOHNS, FRATANTONI, and ZANTOPP, 1993), with some northward recirculation of the southward flow there. This does not appear on the map of total transport but may be seen on the maps at 2000 decibars and deeper (Figs. 8g-8l) and along the bottom (Fig. 3).

Various versions of the transport of the overflows and exchanges north of 50°N have been reviewed by McCARTNEY and TALLEY (1984). They propose a new pattern of flow and a box model to balance the heat and salt transport. The results reported here cannot be compared with their results north of Iceland, but in the Labrador Basin their transports seem to be somewhat less than those estimated here. In earlier studies WORTHINGTON and VOLKMANN (1965) dealt only with the water denser than 27.8 in σ_0 being formed in the North Atlantic as the result of the two Norwegian-Greenland Sea overflows. They took no account of the Mediterranean outflow at that time, as they were concerned with getting the water down rather than accounting for its characteristics farther downstream. Later WORTHINGTON and WRIGHT(1970) showed a Mediterranean contribution down to much higher densities. McCARTNEY (1992) has pointed out that the overflows east and west of Iceland are too small to provide all of the

14 x $10^6 m^3 s^{-1}$ of southward flow that they estimate across 50°N at the western boundary, and that some input from the south is required. The southward flows estimated here are substantially larger, especially south of Cape Hatteras, and must include a major addition of offshore waters.

The northward flow along the eastern boundary in these results has been found in some models. SCHOPP and ARHAN (1986) and ARHAN (1987) show a northward flow along the eastern boundary and noted earlier studies that revealed such a flow. FUKUMORI (1991) modelled the region west of 19°W and found the flow to be anticyclonic at 500 m and cyclonic around the layer of maximum salinity near 1200 m to 1300 m. However, he did not investigate the flow along the eastern boundary, which was to the east of his study.

HOGG (1987) modelled the flow of the Mediterranean salt tongue west of 23°W on two isopycnals. He found the flow in the upper thermocline (about 750 m) to be west-southwestward and at the depth of the salinity maximum (about 1300 m) to be westward and along the axis of the tongue, but he did not deal with the flow along the eastern boundary.

There is some deep northward flow east of the Mid-Atlantic Ridge seen in inverse models, but it is much smaller than that shown here. RINTOUL (1988) and RINTOUL and WUNSCH (1991) used the lines along 24°N and 36°N taken by ROEMMICH and WUNSCH (1985) and considered the balances of the nutrient transports. While their flow field is much like that of ROEMMICH and WUNSCH (1985) they find a very large southward transport of silica across both lines (138 and 152 kmols s^{-1}). To constrain their model to zero transport of silica would require 2 x $10^6 m^3 s^{-1}$ of northward flow of the high-silica water in the eastern part of the section balanced by 2 x $10^6 m^3 s^{-1}$ of southward flow of low-silica water in the west, which they find to be an implausibly large modification to their model.

BOGDEN (1991) finds substantial deep northward flow along the eastern boundary returning southward along the eastern slope of the Mid-Atlantic Ridge, much like these results. However, the net flow along the eastern boundary is southward in his model.

8. THE PRINCIPAL SOURCES AND THEIR EXTREMA

The North Atlantic exchanges waters with the Arctic Ocean, the marginal seas, and the South Atlantic. It receives shallow waters of low temperature and salinity from the Arctic Ocean through the Norwegian-Greenland Sea and through Baffin and Hudson bays, and a shallow layer of warm and saline water from the South Atlantic along the coast of South America.

Warm and saline surface waters flow from the North Atlantic into the Norwegian-Greenland Sea through two passages between Greenland and Scotland (Figs. 4a-b). The waters entering east of Iceland toward the Norwegian Current are cooled and mixed with the deeper and denser Norwegian Sea waters (WORTHINGTON, 1970). A mixture of these waters pours back into the Atlantic as a dense layer that extends down to 3000 m but is still relatively warm and saline (LEE and ELLETT, 1965).

West of Iceland the northward transport is not so warm and saline. It does not alter the Norwegian-Greenland Sea waters so much where it mixes with them at the top of the sill. The waters from the north remain cold, low in salinity, and high in density as they spill downward from the Denmark Strait. They reach the bottom and supply the abyssal layer of the Irminger and Labrador basins.

Near-surface waters also flow from the Atlantic into the Mediterranean Sea. Evaporation and cooling reduce their temperature there and raise the salinity. The density becomes so high that the outflow is dense enough for the characteristics to penetrate to great depths west of the Strait of Gibraltar. Although the highest salinity from the outflow offshore from the sill is found at about 1000 m to 1100 m, the outflow makes the waters between about 30°N and 40°N in the eastern Atlantic the warmest and most saline deep waters (1000 m to 3000 m) not only in the Atlantic (WÜST and DEFANT, 1936), but in the world ocean (LEVITUS, 1982).

Just beneath the warm surface layer the colder and less saline circumpolar waters from the South Atlantic cross the equator along the western boundary at depths down to about 1000 m with a vertical

minimum in salinity near 800 m. The deeper circumpolar waters cross the equator at all depths below 1500 m, as shown by the maps of salinity along various isotherms (WORTHINGTON and WRIGHT, 1970). Below the Intermediate waters and down to the crest of the Mid-Atlantic Ridge the circumpolar waters cross mostly in the east (Fig. 12b), but at greater depths they flow northward on both sides of the Ridge (Fig. 17b).

These various waters are of different density ranges and characteristics, and they circulate at different depths and interleave. The circulation in the shallower layers appears to be much as in the other oceans, but at greater depths the Ridge divides the North Atlantic into two long basins, to the east and west. The various layers within the North Atlantic Ocean are illustrated on vertical sections. One is a composite meridional section (Fig. 5) beginning in the Weddell Sea at 76°S and extending northward through the deeper part of the western basins and the Denmark Strait into the Norwegian-Greenland Sea at about 75°N. The others are zonal sections (Figs. 6 and 7) along 24°N (adapted from ROEMMICH and WUNSCH, 1985) and about 47°N (courtesy of ROSS HENDRY). The vertical section across the Florida Current, which would complete the 24°N section to the coast, is not reproduced here but can be seen in ROEMMICH and WUNSCH (1985). There are other pertinent vertical sections of characteristics that would be useful here. They include the IGY sections (FUGLISTER, 1960), the Erika Dan sections along 53°N and 59°N (WORTHINGTON and WRIGHT, 1970), along 36°N (ROEMMICH and WUNSCH, 1985), along 53°W (KNAPP and STOMMEL, 1985), along 64°W (KNAPP, 1988) and along 25°W (TSUCHIYA, TALLEY, and McCARTNEY, 1992).

The principal layers, from the pycnocline down, are:

the vertical minimum in salinity from the South Atlantic found from 45°S to beyond 16°N at about 800-900 m (Fig. 5b),

the layer of maximum salinity that extends over most of the Atlantic Ocean: it is highest in the region of the Mediterranean outflow near 1100 m (Fig. 6b) and extends across the equator at about 2000 m (Fig. 5b),

the Labrador Sea water which convects to about 1500 m and is cold, low in salinity and nutrients and high in oxygen, and extends eastward across the Atlantic near 1500-1800 m depth (Fig. 5).,

the thick mid-depth layer of oxygen-rich and nutrient-poor water of the central North Atlantic (Fig. 5d-5g and 6d-6h) extending southward across the equator along the western boundary,

and the abyssal layers from the South Atlantic and from the Denmark Strait (Fig 5a); both are cold and low in salinity, but the southern waters are much lower in oxygen and much higher in nutrients (Fig. 5b-5g),

In addition to these layers there is a thick layer of circumpolar water entering from the South Atlantic. It is lower in salinity, temperature, and oxygen and higher in nutrients than the waters flowing southward from the western North Atlantic. Where these two layers meet at about 40°S to 50°S, near the western boundary, the North Atlantic layer penetrates the circumpolar water, splitting it into an upper and a lower layer (Fig. 5), with the North Atlantic water in between (Reid, Nowlin, and Patzert, 1977).

The minimum in oxygen and maxima in nutrients found north and south of the equator in the Atlantic (Figs. 10-16) are, like their counterparts in the Pacific, a consequence of the cyclonic pattern of the baroclinic flow field (DEFANT, 1941a and 1941b; REID, 1989; GORDON and BOSLEY, 1991). In the North Atlantic the lateral extrema extend from the pycnocline down to 3500 m. KAWASE and SARMIENTO (1986) have noted these patterns on a set of isopycnals in σ_2 from about 1000 m to 3300 m in mid latitudes. They account for the area of the oxygen minimum and nutrient maxima in terms of nutrient regeneration.

9. THE INTERMEDIATE WATER

The salinity minimum (Wüst's Subantarctic Intermediate Water) reaching northward beneath the surface from about 50°S (Fig. 5b) extends to at least 16°N all across the Atlantic, where it encounters the upper part of the saline layer from the Mediterranean near 20°N and weakens. It is only marginally present all along 24°N, and is not found farther north.

South of 35°S, which is about the east-west axis of the anticyclonic gyre at 800-1000 m, the salinity minimum lies just at or beneath an oxygen maximum and 400 m to 600 m above nutrient maxima (Figs. 5d-5g). North of 35°S, where westward flow of the gyre is joined by waters from the eastern tropical cyclonic gyre (Fig. 8d), oxygen concentration decreases and the nutrients increase. The flow turns northward along the western boundary and across the equator, but some of it turns eastward just south of the equator (Figs. 8d and 8e), and carries water of low salinity to the eastern boundary. It crosses the equator in the east and the salinity minimum can be found as far as 16°N all across the Atlantic. There is a similar contribution of oxygen-poor nutrient-rich waters near 10°N to 15°N from the eastern North Atlantic. This results in lateral extrema of the eastern characteristics near 10°N.

Though the salinity minimum disappears at about 24°N, waters of this density continue to flow northward (TSUCHIYA, 1989). They contribute high nutrients and low oxygen to the Gulf Stream and North Atlantic current.

10. THE MEDITERRANEAN SEA OUTFLOW

Cooling and loss of heat and water by evaporation reduce the temperature of the Mediterranean Sea and increase its salinity and density, and deep convection occurs (MEDOC Group. 1970). The excess of evaporation over precipitation in the Mediterranean Sea is balanced by an inflow of surface water from the North Atlantic through the Strait of Gibraltar. Beneath the inflowing Atlantic water there is an outflow of the denser Mediterranean water. OCHOA and BRAY (1991) have calculated $0.7 \times 10^6 m^3 s^{-1}$ of outflow at a salinity of 38.4. The earlier estimates that they noted range from $1.34 \times 10^6 m^3 s^{-1}$ at 37.75 to $0.57 \times 10^6 m^3 s^{-1}$ at 37.70. Their own estimate is among the lowest in transport of both water and salt. This outflow is the only source for the maxima in heat and salt content found beneath the thermocline in the Atlantic.

The Mediterranean water first appears in the Atlantic as a salinity maximum starting from about 1100 m off the Strait of Gibraltar, but various maps (WÜST and DEFANT, 1936; WORTHINGTON and WRIGHT, 1970; LEVITUS, 1982) show the Strait as a point source of heat and salt at all depths from 1000 m to more than 2500 m. It extends as tongues of warm and saline water both northward along the coast of Europe and westward across the Atlantic on all of the isopycnals from 31.938 in σ_1 (Fig. 11) to 41.44 in σ_3 (Fig. 15). This flow pattern is seen on all of the maps of steric height from 800 db (Fig. 8d) to 2500 db (Fig. 8h).

This outflow spills down into the northward flow along the eastern boundary which is made up of circumpolar water of lower temperature that has crossed the equator, passed eastward along 10°N to 20°N, and turned northward along the eastern boundary (Figs. 12b-15b and 8d-8i). Its salinity increases along the eastward path as its flow is parallel and opposed to the westward flow of more saline water on its northern side. It reaches a maximum where it receives the spill down from the Strait of Gibraltar. Where it reaches 35°N to 45°N it carries high salinity and temperature both northward along the eastern boundary and westward across the Atlantic. As it nears the western boundary it provides warm water of high salinity to the Gulf Stream at all depths from 700 m to more than 2500 m and to the southward flow off Cape Hatteras, where it raises the temperature and salinity of the flow at depths from 1500 m down to the crest of the Mid-Atlantic Ridge.

Not all of the warm and saline water flowing westward between about 25°N and 45°N in mid-ocean reaches the Gulf Stream or the southward flow along the western boundary. Some part of it turns back eastward between about 15°N and 25°N as part of the cyclonic gyre. Where it turns northward along the

eastern boundary and past the Iberian peninsula it returns some part of the heat and salt injected there by the outflow. The cyclonic gyre acts to maintain the high heat and salt content of the westward and northward tongues which make the Atlantic so warm and saline.

The outflow from the Mediterranean is only about 0.7 x $10^6 m^3 s^{-1}$. This is a very small transport, but the salinity of 38.4 and temperature of 13°C of the outflow are extremely high compared to any other waters in that depth and density range. The effect of these increments is twofold. First, they identify both a northward flow along the eastern boundary to the Greenland-Scotland sill and a westward flow across the Atlantic that turns southward along the western boundary and into the Antarctic Circumpolar Current and the Weddell Sea. Second, even in the distant places where they lie shallow or outcrop near Iceland and in the Weddell Sea, they retain salinities high enough to form the densest waters of the northern North Atlantic and the Weddell Sea.

11. THE LABRADOR SEA

The Labrador Sea receives cold and low-salinity surface water from the Arctic through the East Greenland Current and Hudson and Baffin bays (Figs. 4a and 4b). North of 30°N the upper 2500 m of the Labrador Sea are the coldest and least saline of the North Atlantic (LEVITUS, 1982). The cyclonic flow within the Labrador-Irminger-Iceland basins extends to the bottom in more than 3000 m (Fig. 8i), and brings warmer and more saline water from the east into the Labrador Sea along the northern boundary. Colder and less saline but denser water spills through the Denmark Strait into the Irminger and Labrador basins.

Convection takes place in some years (LAZIER, 1973; CLARKE and GASCARD, 1983). The maximum depth of overturn is estimated to be about 1500 m. The resulting upper layer has salinities near 34.9 and potential temperatures near 3.4°C in θ at about 1000 m (Fig. 5a), and density about 27.75 - 27.78 in σ_0. Down to the depth of convection the characteristics of the Labrador Sea water are low temperature, salinity, and nutrients, and high oxygen. Cross-isopycnal mixing extends these characteristics into water somewhat deeper than the 27.75 to 27.78 in σ_0 of the convecting layer. This upper layer has oxygen concentrations of 6.5 to 7 ml/l (Fig. 5d), and the concentrations remain above 6 ml/l all the way to the bottom. At all depths below 500 m the oxygen concentrations in the Labrador Basin are the highest of the world oceans. Waters with these characteristics extend from the Labrador Sea eastward across the Atlantic with the North Atlantic Current. On the section along about 47°N (Fig. 7) they are recognized between about 1200 m ($\sigma_{1.5}$ 34.64) and 2200 m (σ_2 36.98) by minima in salinity, nitrate and silica, and maxima in oxygen. The overlying waters with higher salinities and nutrients and lower oxygen are from the waters flowing northward with the Gulf Stream and into the North Atlantic Current, and from the poleward flow along the eastern boundary.

The Labrador Sea waters also extend southward along the western boundary, where they are marked by minima in nutrients and a maximum in oxygen along 24°N (Figs. 6e and 6f). Part of this southward flow turns back northward near Cape Hatteras, joining the Gulf Stream and spreading through the anticyclonic gyre (Fig. 13b). WÜST (1935) showed the southward extension of high oxygen from the Labrador Basin on the map representing his Middle North Atlantic Deep Water at 2000-2500 m. This was the first evidence of a deep southward flow that is continuous along the western boundary to about 45°S.

12. THE CIRCUMPOLAR WATER

A substantial amount of circumpolar water enters the North Atlantic from the south at all depths below that of the Intermediate Water. Circumpolar water is defined as the water flowing eastward through the Drake Passage (REID, 1989; REID and MANTYLA, 1989). The density range there is from about 27.0 in σ_0 to about 46.07 in σ_4.

In the open Atlantic water denser than 46.07 in σ_4 is formed only in the Weddell Sea (Fig. 5c). These higher densities extend around Antarctica almost to the Drake Passage, but northward only to the Brazil, Mozambique, and Crozet basins. The abyssal densities of the rest of the open world ocean fall into the density range of the circumpolar water (MANTYLA and REID, 1983).

The shallowest and deepest parts of the circumpolar water in the Drake Passage show the characteristics expected of the high southern latitudes: they are cold and low in salinity. However, in the middle range they contain a salinity maximum (SIEVERS and NOWLIN, 1984). This is the remnant of the warm and saline waters from the North Atlantic that have joined the Antarctic Circumpolar Current, passed eastward around Antarctica, and are returning through the Drake Passage.

The warm and saline water flowing southward along the western boundary has a density range near 30°S from about 27.6 in σ_0 to 45.907 in σ_4, well inside the density range of the circumpolar water. This water meets and mixes with the northward-flowing circumpolar water near 40°S in this density range (Figs. 8e-8k). Near the western boundary it splits the colder circumpolar water from the Drake Passage vertically into two layers of lower salinity, above and below (Fig 5b). Some of the mixture turns back northward as part of the anticyclonic gyre and carries a mixture of the Drake Passage salinity maximum and the western boundary maximum northward toward the North Atlantic. Some part of it turns eastward near the equator and southward along the eastern boundary and joins the Antarctic Circumpolar Current south of Africa (Figs. 8f-8i and 13b). This mixture provides the salinity maximum that is observed in the eastward flow all around Antarctica and in the southern parts of the Indian and Pacific oceans (REID and LYNN, 1971).

13. THE DEEPER PENETRATIONS

The open North Atlantic does not form surface waters dense enough to sink by vertical convection to more than the 1500 m observed in the Labrador and Irminger seas. This became apparent from the work of LEE and ELLETT (1965 and 1967) and WORTHINGTON and WRIGHT (1970). WORTHINGTON's (1976) study of the open North Atlantic circulation did not require overturn to greater depths. However, some of the warm and saline waters from the open Atlantic flow into the Norwegian-Greenland Sea where they become cold and dense enough to convect to the bottom (Fig. 5). The denser waters pass back through shallow channels east and west of Iceland into the open Atlantic. As they cross over the sills they mix with the warmer overlying Atlantic waters but are still dense enough to spill down the slopes into the Atlantic basins (WORTHINGTON, 1970 and 1976; WORTHINGTON and WRIGHT, 1970). The various steps in learning the origin of these dense waters have been discussed by WARREN (1981) in his account of the deep circulation of the world ocean.

East of Iceland waters from the North Atlantic Current, the Labrador Sea, and the poleward flow along the eastern boundary, reach the Iceland-Scotland sill. At the sill they mix with the denser overflowing Norwegian Sea waters, and their mixture pours southwestward across the sill down to more than 3000 m, above the deeper circumpolar water (STEELE, BARRETT and WORTHINGTON, 1962; LEE and ELLETT, 1965, 1967; IVERS, 1975). The mixture of these various sources that is found in the northern Iceland Basin extends along and around the Reykjanes Ridge at all depths from below the Intermediate Water down to the sill at the Charlie Gibbs Fracture Zone (Figs. 13-16), where it turns northward from there into the Irminger Basin. It alters the characteristics of the deepest circumpolar water entering from the South Atlantic and provides the characteristic signatures — high heat and salt content — of the deeper waters flowing southward along the boundary and into the South Atlantic.

West of Iceland a similar flow of warm and saline waters into the Norwegian-Greenland Sea takes place, and below it the very dense cold water from the intermediate and upper layers of the Norwegian-Greenland Sea flows southward through the Denmark Strait (STEFANSSON, 1962; SWIFT, AAGAARD, and MALMBERG, 1980; SWIFT, 1984; DICKSON, GMITROWICZ and WATSON, 1990). Vertical mixing takes place, just as in the overflow east of Iceland, but its temperature remains lower than that of the eastern overflow. This may be because the northward transport of the warm Atlantic surface

waters on the west side of Iceland, with which the outflowing waters mix, is not as great as that across the sill east of Iceland. The waters flowing south from the Denmark Strait are colder than those flowing south from the Faeroe Bank Channel, and are thus more compressible. They will have a higher density increment imposed upon them as they flow downward into higher pressures. For whatever reason, the waters that pass downward into the Irminger Sea remain denser, colder, and less saline than the surrounding waters as they reach the bottom near 57°N. Their density there, even after mixing, is still more than 46.00 in σ_4 in the Irminger and Labrador seas. This is about the same as that of the bottom of the circumpolar water that crosses the equator into the North Atlantic west of the Ridge.

On the vertical section at 47°N illustrated here (Fig. 7b), and particularly on the sections prepared by WORTHINGTON and WRIGHT (1970) the Iceland Basin mixture is seen as a salinity maximum all across the Iceland and Irminger basins. The highest values are next to the Ridge, on both sides, at depths near 2500 m. In the Iceland Basin it lies above the less saline, lower oxygen bottom waters from the south. In the Irminger Basin it is above the overflow waters from the Denmark Strait, which are less saline (REID and LYNN, 1971). It passes below the salinity minimum and oxygen maximum of the Labrador Sea.

14. THE PATTERNS ALONG ISOPYCNALS

14a. The isopycnal where $\sigma_0 = 26.75$

The shallowest isopycnal illustrated is 26.75 in σ_0 (Fig. 10). On this and all of the other isopycnal maps the shaded parts represent areas where all the water is less dense than the isopycnal, and the dashed lines indicate outcrops at the sea surface.

This isopycnal outcrops near 40°N and 45°S and lies deepest in the west, a little more than 600 m, between the Gulf Stream and its return flow. The major feature in salinity is the high in the east extending westward from its maximum value at the Strait of Gibraltar. The isopycnal lies shallower than 100 m near the Strait and may receive part of its high salt content from the upper waters of the evaporation cell of the open Atlantic, but the pattern is much the same as seen on the deeper isopycnals. Less saline water from the south crosses the equator in the west and flows into the Caribbean Sea and Gulf of Mexico (SCHMITZ and RICHARDSON, 1991), and less saline waters also flow southward along the western boundary from the Labrador Sea to about 30°N.

The lowest oxygen and highest nutrients are found in the two extrema just north and south of the equator in the eastern Atlantic. These characteristics extend westward into the Caribbean Sea and north of the Antilles. They are carried northward with the Florida Current and upper Gulf Stream, accounting for the lower oxygen and higher nutrients in the west.

14b. The isopycnal where $\sigma_1 = 31.938$

The isopycnal defined by σ_1 = 31.938 (Fig. 11) lies within the Intermediate Water salinity minimum near the equator. The layer extends as a minimum throughout the equatorial zone and to beyond 16°N. The flow appears to be eastward along and just south of the equator (Figs. 8d and 8e). It turns northward in the east and then westward between about 2°N and 8°N. Part of it continues northwestward along the coast of South America and into the Caribbean Sea and Gulf of Mexico and part turns eastward between 10°N and 20°N and back to the eastern boundary. The minimum extends only a little north of 20°N, where the isopycnal lies between the higher salinities of the overlying evaporation cell and the underlying Mediterranean outflow (Fig. 5b). GORDON (1967) and ORTEGA (1972) have traced the Intermediate Water into the Caribbean by its low salinity and HOFFMAN and WORLEY (1986) have traced it into the Gulf of Mexico. In those marginal seas the vertical and lateral density structure and the gradients of characteristics are weak at depths below 1000 m, and no clear pattern of deeper flow has yet emerged.

At the depth of this isopycnal in mid-latitudes the westward limb of the anticyclonic gyre has shifted poleward. The northern part of the westward flow (north of 30°N at 40°W) carries warm and saline waters of moderate oxygen and nutrient content. The southern part (south of 30°N at 40°W) is part of the eastern cyclonic gyre and carries the very low oxygen and very high nutrients of that gyre. The mixing that takes

place along the westward flow accounts for the lower oxygen and higher nutrients that characterize the Gulf Stream as far as 50°N, where they mix with Labrador Sea waters of opposite characteristics (TSUCHIYA, 1989).

The Labrador Basin characteristics of low salinity, high oxygen, and low nutrients circulate within the northern cyclonic gyre and southward along the western boundary to about the latitude of Cape Hatteras. There is some indication of an extension farther south along this isopycnal. Most of the southward flow in the upper layer has turned back northward with the Gulf Stream. Between 20°N and 40°N this isopycnal lies near a layer of oxygen minimum, and the high-oxygen signal is lost. However, the salinity remains low along the boundary and some of the nutrients are low. On the deeper isopycnals, however, the northern signals are clear.

The poleward flow along the eastern boundary carries the low oxygen, high nutrient waters of the eastern tropical zone northward beyond 30°N, where, at this density, they turn westward and southward with the anticyclonic flow of mid-latitudes.

14c. The isopycnal where $\sigma_1 = 32.20$

At the depths where $\sigma_1 = 32.20$ (Fig. 12) the patterns are much the same. There is still a flow of cooler water of low salinity from the south into the Caribbean, but there is no exit at this density through the Straits of Florida. The low-salinity waters appear to cross the equator near the eastern boundary and to flow westward near 5°N-10°N to the western boundary (Fig 8e). Along this isopycnal the Gulf Stream is still made up of waters of the westward limb of the anticyclonic gyre, which include some of the oxygen-poor, nutrient rich waters along the eastern boundary (TSUCHIYA, 1989) and some of the Mediterranean outflow. The high nutrients extend with the Gulf Stream and North Atlantic Current to about 60°N. North of about 35°N they mix with the lower nutrient waters of the Labrador Sea, and in the return flow the nutrients are lower. There is evidence of an eastward flow along the equator in the oxygen and nutrient patterns.

14d. The isopycnal where $\sigma_{1.5} = 34.64$

The isopycnal where $\sigma_{1.5} = 34.64$ (Fig. 13) represents the upper layer of the Labrador Sea. In their study TALLEY and McCARTNEY (1982) used the isopycnal where $\sigma_{1.5} = 34.72$, a little deeper than this, but the patterns are much the same. This isopycnal outcrops north of Iceland and in a small area just south of Greenland and lies deepest (about 1800 m) along the axis of the anticyclonic gyre (Fig. 13a).

The flow along this isopycnal is shown in Fig 13b. With the flow already defined at all depths, laterally summing the increments of steric height between each station pair at the average depth of the isopycnal there produces a field of adjusted steric height along the isopycnal. South of 50°N it is much like the flow at 1500 db and 2000 db (Figs. 8f and 8g) but farther north it shows the flow up to the top of the sills.

This is the first of the mapped isopycnals on which the overflow east of Iceland is seen. On shallower isopycnals the salinity and temperature decrease monotonically northward from the Mediterranean salt tongue into the Norwegian Sea, and there is no obvious indication of any vertical mixture across the sill required to account for the patterns. But where $\sigma_{1.5} = 34.64$ the water flowing southwestward from the sill is warmer and more saline than the waters of this density — the Labrador Sea waters — flowing northward toward the sill (Fig. 13c).

The Norwegian Sea is not a source of high temperature and salinity. The denser waters leaving the Faeroe Bank Channel are colder and less saline than those that entered near the surface, and are only returning part of the heat and salt that has been carried in. On surfaces of constant depth there is only a marginal suggestion of an input of higher temperature and salinity to the northern Iceland Basin (WÜST and DEFANT, 1936; DIETRICH, 1969; LEVITUS, 1982), though the Mediterranean outflow into the Atlantic is obvious. The lack of such a strong signal on maps of constant depth in the Iceland Basin may explain the long delay in recognizing the outflow.

This Iceland Basin mixture flows westward south of Iceland and southward along the Reykjanes Ridge with the cyclonic gyre. It follows the gyral path into Irminger Basin and northward along the Ridge

(Fig. 13b). It turns southward along the coast of Greenland. It can be seen at this density and on vertical sections as a warm and saline flow along the boundary of the Labrador Basin, around the lower salinities of the central Labrador Sea (WORTHINGTON and WRIGHT, 1970; REID and LYNN, 1971). It lies above the colder and less saline waters from the Denmark Strait.

The near-surface waters passing northward to the west of Iceland are not as warm and saline as those to the east. Their mixture with the Norwegian-Greenland Sea waters does not produce more saline and warmer waters in the Irminger Basin on any isopycnal. The waters flowing southward from the Denmark Strait are colder and less saline on all isopycnals, but south of the Strait they mix with the Iceland Basin waters, and the salinity and temperature are raised in the flow around the south of Greenland and the Labrador Basin. The high oxygen and low nutrient content of the Norwegian-Greenland Sea can be recognized in the overflow.

Along this isopycnal, as on all of those from the Intermediate Water down to the sill of the Mid-Atlantic Ridge, the anticyclonic gyre receives part of the Mediterranean outflow and carries it westward. The flow divides as it nears the western boundary. Part of it turns northward and becomes part of the deep Gulf Stream. Part turns southward along the western boundary. At this density, and down to 41.44 in σ_3, the warmest and most saline waters of both the Gulf Stream and the southward flow are found offshore south of Cape Hatteras, where the westward limb of the gyre, carrying part of the Mediterranean outflow, joins these flows. This is the shallowest of the isopycnals where the salinity, oxygen, and nutrient patterns indicate that the southward flow along the western boundary extends south of Cape Hatteras (see Figs. 8f and 8g).

The eastward flow along the equator, though it cannot be represented clearly by the maps of geostrophic flow, is indicated by patterns of all of the characteristics (Figs. 13c-13f) including freon (WEISS, BULLISTER, GAMMON, and WARNER, 1985). The salinity field indicates that the source is not from the north alone, but has an eastward component from south of the equator, some of which turns northward in the east and westward near 10°N to 20°N. This is circumpolar water, and it accounts for the low salinity on this isopycnal between the equator and the high-salinity from the Mediterranean outflow. The northward flow along the eastern boundary is indicated by the oxygen and silica fields as far as 60°N, though the high salinity signal is mixed away near 50°N by the Labrador Sea water.

14e. The isopycnal where $\sigma_2 = 36.98$

Where $\sigma_2 = 36.98$ (Fig. 14) the same general patterns of circulation obtain (Fig. 8g), but this is well below the depth of the Labrador Sea convection. The low-salinity signal of the Labrador Sea water still extends eastward along about 50°N but it is higher than at 34.64 in $\sigma_{1.5}$. The characteristics of the northward flow along the eastern boundary are more evident in the eastern part of the northern cyclonic gyre. The Rockall Trough appears to be dominated by waters from the south. Oxygen concentrations are lower and nutrients higher than those to the west throughout most of the cyclonic gyre, though the water spilling southward east of Iceland is still high in oxygen and low in nutrients. The high salinity of the Iceland Basin mixture is clearly present in the Irminger Sea, though the Denmark Strait waters are still high in oxygen and low in nutrients.

The westward limbs of the anticyclonic gyre and the cyclonic gyre in the south still carry the high salinity and nutrients and low oxygen westward. They feed into both the deep Gulf Stream and the southward flow along the western boundary. Along this isopycnal the warmest and most saline segments of both the Gulf Stream and the southward flow are still found near 20°N to 30°N, between the lower salinity waters from the Labrador Basin and the circumpolar waters that have crossed the equator in the east. The eastward flow along the equator is reflected in the patterns of characteristics, and the salinity pattern indicates that some of the flow turns northward across the equator in the east.

14f. The isopycnal where $\sigma_3 = 41.44$

Where σ_3 = 41.44 (Fig. 15) the warm water spilling southwestward east of Iceland is even more dominant within the northern gyre. It extends into the central Labrador Basin offshore of the narrow stream of Denmark Strait water that flows around the south of Greenland and the Labrador Basin. The overflow west of Iceland is best shown by the high oxygen and low salinity and nutrients.

The Mid-Atlantic Ridge partly restricts the zonal flow north of about 35°N on this isopycnal. The southwestward parts of the two gyres (Fig. 8h) pass on both sides of the Azores Plateau, and the more saline part passes westward south of the Plateau. They still provide the warmest and most saline segment of the Gulf Stream and of the southward flow along the western boundary near 30°N, but the values are not much higher than the Iceland Basin mixture where it has reached the western Labrador Basin. The oxygen concentration is lower in the northern part of the eastern basin than in the waters above, and the nutrients higher.

There is still evidence of eastern flow along the equator though it does not seem so strong. The salinity pattern suggests a broader band of circumpolar water crossing the equator in the east and turning both westward toward the deep Gulf Stream and northeastward along 20°N toward the eastern boundary.

14g. The isopycnal where $\sigma_3 = 41.50$

The isopycnal defined by σ_3=41.50 extends from the sea surface to almost 3500 m (Fig. 16a). The flow along this isopycnal is mapped in Fig. 16b in the same manner as in Fig. 13b. In low latitudes, where the surface is more nearly horizontal, the flow is much like those at 3000 and 3500 db (Figs. 8i and 8j). However, in the far north only the map of flow along the isopycnal can trace the flow both up to and down from the passages east and west of Iceland.

The Charlie Gibbs Fracture Zone (near 53°N 33°W) is the deepest passage through which the Iceland Basin mixture can flow westward into the Irminger Basin (Fig. 16b). Waters of this density flowing westward through the Zone show the high salinity characteristic of the spill, but the eastern boundary still shows the lower oxygen and higher nutrients of the northward flow. There is some penetration of the Iceland Basin mixture southward past the Zone into the eastern basin, as noted by LEE and ELLETT (1965). The higher salinity from the Iceland Basin mixture extends westward through the Zone into the eastern Irminger Basin and the central Labrador Basin, but the western Irminger Basin and the perimeter of the Labrador Basin at this density show more of the low salinity and high oxygen of the Denmark Strait overflow.

At this density the low salinity of the circumpolar water appears to cross the equator over the eastern half of the ocean. It extends northwestward as part of the deep Gulf Stream and can be traced to about 50°N, where it meets the Iceland Basin mixture, with its higher salinity and oxygen. There is no clear and direct input of warm and saline Mediterranean outflow off the Strait of Gilbraltar along this isopycnal. The highest salinity in the eastern basin is in the north, from the Iceland-Scotland overflow. At this and greater densities the waters within the central Labrador Basin have the highest salinity seen in the western basin; the maximum is no longer from the Mediterranean outflow but from the Iceland Basin mixture, through the Labrador Sea.

14h. The isopycnal where $\sigma_4 = 45.88$

The three deepest isopycnals (45.88, 45.907 and 45.92 in σ_4) (Figs. 17, 18, and 19) extend from the Norwegian-Greenland Sea to the western basin through the Denmark Strait, but are too dense to extend across the Reykjanes Ridge to the Iceland Basin. They are seen there in a separate pool just south of Iceland along the eastern slope of the Reykjanes Ridge, not continuous on these isopycnal maps with the overflow east of Iceland. The data used are from the first survey of the Overflow Expedition of May-June 1960 (TAIT, LEE, STEFANSSON and HERMAN, 1967), and perhaps the period of maximum overflow had passed. (The stations over the sill are so closely spaced that they cannot be shown here, but they were used in the contouring.) Alternatively the discontinuity may result from the method of tracing, which cannot deal properly with the cross-isopycnal mixing that takes place over the sill.

The isopycnal where σ_4 = 45.88 (Fig. 17) is not continuous across the Mid-Atlantic Ridge from the Iceland Basin to the Labrador Basin. However it still shows the effect of the Iceland Basin mixture in the central Labrador Basin, where vertical diffusion from the overlying less dense layers of the mixture has raised the temperature and salinity down to this isopycnal. The colder and less saline overflow from the Denmark Strait, with high oxygen, extends around the perimeter of the Labrador Sea.

There is still at this density some eastward flow near the equator, but it appears to be limited by the Mid-Atlantic Ridge to a narrower flow just south of the equator (TSUCHIYA, TALLEY, and McCARTNEY, 1992). The lower salinity circumpolar water extends into the North Atlantic on both sides of the Mid-Atlantic Ridge. There appears to be some flow at this density westward through the Vema Fracture Zone near 11°N, though the underlying flow is eastward (WÜST, 1935; MANTYLA and REID, 1983; McCARTNEY, BENNETT and WOODGATE-JONES, 1991; SPEER and McCARTNEY, 1991) and carries slightly denser water (about 45.90 in σ_4, θ=1.68°C) through the Fracture Zone (Fig. 20).

In the eastern basin this isopycnal does not extend north of about 30°N. The salinity and oxygen are quite low, and the nutrients high. In the western basin the lower salinity of the circumpolar water extends northward along the Ridge to about 50°N, where it meets the high salinity and temperature diffused down from the overlying Iceland Basin mixture. The higher salinities extend southward from the Labrador Sea along the western boundary, with their characteristic high oxygen and low nutrient values. Within the eastern basin the flow is weak and appears to retain a cyclonic pattern down to 4500 decibars (Fig. 8l), as suggested by LONSDALE (1982) and DICKSON, GOULD, MÜLLER, and MAILLARD (1985).

14i. The isopycnal where σ_4 = 45.907

The deepest isopycnal that extends continuously from the Weddell Sea to the Labrador Sea is where σ_4 = 45.907 (Fig. 18). It lies deepest and touches the bottom at about 5200 m near 39°N, just south of the Grand Banks of Newfoundland. It extends east of the Mid-Atlantic Ridge a short distance through the Romanche Fracture Zone. The circumpolar waters extend northward along the western flank of the Ridge, and near 20°N to 25°N a part of them spreads westward south of the Bermuda Rise (WÜST, 1935; McCAVE and TUCHOLKE, 1986).

Where this isopycnal lies shallower north of 40°N the flow is still southward along the western boundary, carrying the Denmark Strait overflow waters that have been made warmer and more saline near 50°N by the Iceland Basin mixture. This southward flow appears to be blocked at about 5000 db by the rise extending northwestward from Bermuda, and to turn back northward (Fig. 8m). The characteristics, however, suggest that the waters just south of the Rise have received some input from the more saline and oxygen-rich waters from the north. This could come about from some vertical exchange with the slightly less dense overlying waters that are moving southward above the Rise.

14j. The isopycnal where σ_4 = 45.92

Waters of 45.92 in σ_4 (Fig. 19) are formed in both the North and South Atlantic but they do not meet along this isopycnal. The only source for waters of this density in the Labrador and Irminger basins is the cold and less saline water flowing over the Denmark Strait. The higher values of salinity (temperature) and oxygen in the Labrador Basin must result from vertical exchange with the overlying Iceland Basin mixture, which has crossed the Reykjanes Ridge at lower densities.

The salinities (and temperatures) of both the circumpolar water from the south and the Denmark Strait water increase as they extend toward each other along this isopycnal (Fig. 19b). This is also true of the abyssal temperature (Fig. 20) and salinity (MANTYLA and REID, 1983). These alterations are the result of the vertical exchanges which decrease the density of the deeper water. Water is moving not only along but through this isopycnal. Both the Denmark Strait water and the circumpolar waters are becoming warmer and less dense as they approach each other, and there is no reason to suppose that such mixing is confined to the deeper waters. Hence none of the patterns on any of the isopycnals illustrated herein can be the result of lateral mixing alone, but must reflect some effect of vertical exchange. While they cannot represent surfaces to which the flow is restricted they may be taken as useful approximations. Material surfaces do not exist in the ocean.

The southward flow along the western boundary appears to be continuous from the Labrador Basin to the South Atlantic at all depths from a little above 1500 m down through 4500 m (Fig. 81). Below 4500 m (Fig. 18) the southward flow does not appear to cross the Bermuda Rise, but to turn offshore and northward in a small and separate gyre. It may be the deepest expression of the great cyclonic gyre which is confined to the western basin below 3000 m by the Mid-Atlantic Ridge. South of the Bermuda Rise the deep characteristics (Figs. 18 and 19) show that the low salinity and oxygen and high silica from the south are still being affected by the overlying northern waters.

15. SUMMARY

Along the western boundary of the Atlantic Ocean there is a deep southward flow extending from about 60°N to its junction with the Falkland Current near 45°S, where it turns offshore (Figs. 5 and 13-18). Although the North Atlantic receives warm surface waters from the South Atlantic along the western boundary, and cold and low-salinity surface waters from the Arctic Ocean through the Norwegian-Greenland Sea and Baffin Bay, these waters do not directly provide the denser waters of the southward flow by convection to the bottom. The deepest open-ocean penetration of surface water by convection is in the Labrador and Irminger seas, to about 1500 m.

The greater part of the water leaving the North Atlantic and passing southward through the South Atlantic is made up of circumpolar water that has crossed the equator from the south, that is, water with the characteristics and density of the waters passing around Antarctica and through the Drake Passage. This incoming water is cooler, less saline, lower in oxygen and higher in nutrient content than the water flowing out, but its density range encompasses that of the waters that cross the equator southward. It enters the North Atlantic at all densities from the Intermediate Water to the bottom, circulates through the major gyral systems, is joined by three overflows from the marginal seas, and returns southward with its characteristics altered.

The Mediterranean outflow is the source of the mid-depth increments of heat and salt to the waters entering the North Atlantic. As it pours down from the Strait of Gibraltar it joins the subsurface waters flowing northward along the eastern boundary. These include waters from the South Atlantic, and until they receive the outflow they are relatively low in temperature and salinity. They carry the outflow northward to about 40°N and divide, part continuing northward along the boundary toward Iceland and part turning westward with the westward limbs of the large cyclonic and anticyclonic gyres. The northward part carries warm and saline water that mixes with the Norwegian-Greenland Sea waters in the passages east and west of Iceland. The westward part crosses the Atlantic, and as it approaches the western boundary near 25° to 35°N it turns both northward, forming the deeper part of the Gulf Stream above about 3000 m, and southward, joining the southward flow along the western boundary and the eastward limb of the cyclonic gyre. As a result of these gyral flows the added heat and salt from the Mediterranean outflow are spread both northward toward the cyclonic gyre of the north and southward along the western boundary and into the South Atlantic Ocean, where their contributions make the southward flow warmer and more saline than the incoming circumpolar waters to the east.

The waters that flow southward over the Iceland-Scotland sill into the northern Iceland Basin are a mixture of the very dense Norwegian Sea waters at the sill with the less dense but very warm and saline waters of the open Atlantic. These include those that have come northward along the eastern boundary carrying part of the Mediterranean outflow. They are at all depths warmer and more saline than those of the Irminger and Labrador basins. At densities from 41.44 in σ_3 to the bottom they are the warmest and most saline of the entire North Atlantic. The mixture pours downward along the continental slope to depths as great as 3200 m. In the eastern basin it passes southward along the Reykjanes Ridge, westward through the Charlie Gibbs Fracture Zone, and cyclonically around the Irminger and Labrador basins, bringing warmer and more saline water into the western basin.

Only the third overflow, from the Denmark Strait, includes waters dense enough to reach the bottom at depths as great as 4000 m. They provide the only North Atlantic abyssal water that is as dense as the densest incoming circumpolar water at the equator. This very dense cold water from the Norwegian-Greenland Sea pours along the bottom into the Irminger Sea, passes westward just south of Greenland, loops cyclonically around the Labrador Sea, and then southward along the western boundary. Although it mixes along its path with the overlying warmer, less dense and more saline water that has passed westward over and through the Charlie Gibbs Fracture Zone, it can still be recognized along the bottom by its low temperature and high density to about 40° to 45°N. Here at the bottom it meets abyssal circumpolar water from the south, which at this latitude has been mixed to the same density and nearly the same temperature and salinity. The warmest, most saline, and least dense abyssal waters of the western basin are found here where the remnants of the Denmark Strait and the circumpolar waters meet.

A deep layer of warm and saline water is formed in the North Atlantic Ocean. It extends southward along the western boundary in the South Atlantic and then eastward around Antarctica. Its distinguishing characteristics are not formed by convection of warm and saline water within the open North Atlantic, but by overflows from the Mediterranean and Norwegian-Greenland seas. The rates of flow of these spills are not great enough to provide by themselves the amount of water that flows southward along the western boundary and into the South Atlantic. Instead, the particular characteristics — the high temperature and salinity — of the deeper waters from the North Atlantic that extend into the other oceans, are achieved by adding the spills from the Mediterranean and Norwegian-Greenland seas to the larger volume of colder and less saline circumpolar waters that flow northward from the Antarctic Circumpolar Current. The heat and salt added from the Mediterranean source do not flow out in a simple southward stream. Instead they take part in the system of gyral flows in the North Atlantic before departing southward, and their residence time in the North Atlantic makes it the warmest and most saline of the world's oceans.

The warm and saline deep water flowing out of the North Atlantic extends throughout the Antarctic, Indian, and Pacific oceans. Though its other extrema diminish along the flow, it is recognized as a salinity maximum that lies above the bottom over most of the southern hemisphere and extends back into the Atlantic Ocean through the Drake Passage. Although the salinity decreases along the flow it remains high enough where the saline layer outcrops or lies shallow in the Weddell Sea to contribute to the formation of the densest abyssal water of the open world ocean.

ACKNOWLEDGEMENTS

The work reported here represents one of the results of research supported by the National Science Foundation, the Office of Naval Research, and the Marine Life Research Program of the Scripps Institution of Oceanography. I wish to acknowledge the assistance given by Arnold Mantyla in selecting the data, by Sarilee Anderson in arranging the data and calculating and plotting the data points along the isopycnals and on the fields of steric height through the long succession of adjustments, and by David Newton for writing the various programs. I thank Ray Peterson, Mizuki Tsuchiya, Lynne Talley, and Arnold Mantyla for reading and commenting upon the manuscript.

REFERENCES

ARHAN, M. (1987) On the large scale dynamics of the Mediterranean outflow. *Deep-Sea Research*, **34**, 1187-1208.

ARNAULT, S., A. MORLIERE, J. MERLE, and Y. MENARD (1992) Low frequency variability of the tropical Atlantic surface topography: Altimetry and model comparison. *Journal of Geophysical Research*, **97**, 14,259-14,288.

BARTON, E. D. (1989) The poleward undercurrent on the eastern boundary of the subtropical North Atlantic. In: *Poleward Flows Along Eastern Boundaries*, S. J. Neshyba, Ch. N. K. Mooers, R. L. Smith, and R. T. Barber, editors, Springer-Verlag, NY, 82-95.

BOGDEN, P. (1991) The North Atlantic circulation: Combining simplified dynamics with hydrographic data. *Dissertation, University of California, San Diego, Scripps Institution of Oceanography*, 102 pp.

CLARKE, R. A. (1984) Transport through the Cape Farewell-Flemish Cap section. *Rapports et Procés Verbaux des Reunions Extrait du Journal du Conseil International Pour l'Exploration de la Mer*, **185**, 120-130.

CLARKE, R. A., and J.-C. GASCARD (1983) The formation of Labrador Sea Water. Part I: Large-scale Processes. *Journal of Physical Oceanography*, **13**(10), 1764-1778.

DEFANT, A. (1941a) Quantitative Untersuchungen zur Statik und Dynamik des Atlantischen Ozeans. Die relative Topographie einzelner Druckflachen im Atlantischen Ozean. In *Wissenschaftliche Ergebnisse der Deutschen Atlantischen Expedition auf dem Forschungs—und Vermessungsschiff "Meteor" 1925-1927*, **6** (2)(4),183-190, Beilagen X-XVIII.

DEFANT, A. (1941b) Quantitative Untersuchungen zur Statik und Dynamik des Atlantischen Ozeans. Die absolute Topographie des physikalischen Meeresniveaus und der Druckflachen sowie die Wasserbewegungen im Raum des Atlantischen Ozeans. In *Wissenschaftliche Ergebnisse der Deutschen Atlantischen Expedition auf dem Forschungs—und Vermessungsschiff "Meteor" 1925-1927*, **6**(2)(5), 191-260 Beilagen XIX-XXIX.

DICKSON, R. R., E. M. GMITROWICZ, AND A. J. WATSON (1990) Deep-water renewal in the northern North Atlantic. *Nature*, **344**, 848-850.

DICKSON, R. R., W. J. GOULD, T. J. MÜLLER, and C. MAILLARD (1985) Estimates of the mean circulation in the deep (>2,000 m) layer of the Eastern North Atlantic. *Progress in Oceanography*, **14**, 103-127.

DIETRICH, GUNTER (1969) Atlas of the Hydrography of the Northern Atlantic Ocean. Based on the Polar Front Survey of the International Geophysical Year, Winter and Summer 1958. *Conseil International pour l'Exploration de la Mer, Service Hydrographique*, 140 pp.

EKMAN, V. W. (1934) Review of: Georg Wüst. "Das Bodenwasser und die Gliederung der Atlantischen Tiefsee". *Journal du Conseil*, **9**, 102-104.

FOFONOFF, N. P. (1985) Physical properties of seawater: A new salinity scale and equation of state for seawater. *Journal of Geophysical Research*, **90**, 3332-3342.

FUGLISTER, F. C. (1960) Atlantic Ocean atlas of temperature and salinity profiles and data from the International Geophysical Year of 1957-1958. *Woods Hole Oceanographic Institution Atlas Series* **1**, 209 pp.

FUKUMORI, ICHIRO (1991) Circulation about the Mediterranean Tongue: An analysis of an EOF-based model ocean. *Progress in Oceanography*, **27**, 197-224.

GORDON, A. L. (1967) Circulation of the Caribbean Sea. *Journal of Geophysical Research*, **72**, 6207-6223.

GORDON, A. L., and K. T. BOSLEY (1991) Cyclonic gyre in the tropical South Atlantic. *Deep-Sea Research*, **38**, 5323-5343.

HELLERMAN, S., and M. ROSENSTEIN (1983) Normal monthly wind stress over the World Ocean with error estimates. *Journal of Physical Oceanography*, **13**, 1093-1104.

HOFMANN, E. E., and S. J. WORLEY (1986) An investigation of the circulation of the Gulf of Mexico. *Journal of Geophysical Research*, **91**, 14221-14236.

HOGG, N. G. (1983) A note on the deep circulation of the western North Atlantic: its nature and causes. *Deep-Sea Research*, **30**, 945-961.

HOGG, N. G. (1987) A least-squares fit of the advective-diffusive equations to Levitus Atlas data. *Journal of Marine Research*, **45**, 347-375.

HOGG, N. G. (1992) On the transport of the Gulf Stream between Cape Hatteras and the Grand Banks. *Deep-Sea Research*, **39**, 1231-1246.

HUTHNANCE, J., and W. J. GOULD (1989) On the Northeast Atlantic Slope Current. In: *Poleward Flows Along Eastern Ocean Boundaries*, S. J. Neshyba, Ch. N. K. Mooers, R. L. Smith, and R. T. Barber, editors, Springer - Verlag, NY, 76-81.

IVERS, W. D. (1975) The Deep Circulation in the Northern North Atlantic, with Especial Reference to the Labrador Sea., *Ph.D. dissertation, University of California, San Diego*, 179 pp.

JOHNS, W. E., D. M. FRATANTONI, and R. J. ZANTOPP (1993) Deep Western Boundary Current variability off Northeastern Brazil. *Deep-Sea Research*, **40**, 293-301.

KAWASE, M., and J. J. SARMIENTO (1986) Circulation and nutrients in middepth Atlantic waters. *Journal of Geophysical Research*, **91**, 9749-9770.

KNAPP, G. P. (1988) Hydrographic data from RV Endeavor Cruise 129 (64°W). *Technical Report, WHOI-88-41, Woods Hole Oceanographic Institution*, 111 pp.

KNAPP, G. P., and H. M. STOMMEL (1985) Hydrographic data from RV Oceanus Cruise 133, Leg VII (53°W). *Technical Report, WHOI-85-38, Woods Hole Oceanographic Institution*, 107 pp.

LAZIER, J. R. N. (1973) The renewal of Labrador Sea Water. *Deep-Sea Research*, **20**(4), 341-353.

LEAMAN, K. D., and J. E. HARRIS (1990) On the average transport of the deep water boundary currents east of Abaco Islands, the Bahamas. *Journal of Physical Oceanography*, **20**, 467-475.

LEE, A., and D. ELLETT (1965) On the contribution of overflow water from the Norwegian Sea to the hydrographic structure of the North Atlantic Ocean. *Deep-Sea Research*, **12**, 129-142.

LEE, A., and D. ELLETT (1967) On the water masses of the Northwest Atlantic Ocean. *Deep-Sea Research*, **14**, 183-190.

LEE, T. N., W. JOHNS, F. SCHOTT, and R. ZANTOPP (1990) Western boundary current structure and variability east of Abaco, Bahamas at 26.5°N. *Journal of Physical Oceanography,* **20,** 446-466.

LEVITUS, S. (1982) Climatological atlas of the world ocean. *NOAA Professional Paper 13,* 173 pp.

LONSDALE, PETER (1982) Sediment drifts of the Northeast Atlantic and their relationship to the observed abyssal currents. *Bulletin Institut Geologique Bassin d'Aquitaine, Bordeaux,* **31,** 141-149.

MANTYLA, A. W., and J. L. REID (1983) Abyssal characteristics of the world ocean waters. *Deep-Sea Research,* **30,** 805-833.

McCARTNEY, M. S. (1992) Recirculating components to the deep boundary current of the northern North Atlantic. *Progress in Oceanography,* **29,** 283-383.

McCARTNEY, M. S., S. L. BENNETT, and M. E. WOODGATE-JONES (1991) Eastward flow through the Mid-Atlantic Ridge at 11°N and its influence on the abyss of the Eastern Basin. *Journal of Physical Oceanography,* **21,** 1089-1121.

McCARTNEY, M. S., and L. D. TALLEY (1984) Warm-to-cold water conversion in the northern North Atlantic Ocean. *Journal of Physical Oceanography,* **14,** 922-935.

McCAVE, I. N., and B. E. TUCHOLKE (1986) Deep current-controlled sedimentation in the western North Atlantic. In: *The geology of North America,* **M,** *The western North Atlantic Region.* The Geological Society of America.

MEDOC GROUP (1970) Observations of formations of deep water in the Mediterranean Sea. *Nature,* **227,** 1037-1040.

MERLE, J. (1978) Atlas hydrologique saisonnier de l'Ocean Atlantique Intertropical. *Travaux et Documents de l'O.R.S.T.O.M.,* **82,** 184 pp.

MOLINARI, R. L., R. A. FINE, and E. JOHNS (1992) The Deep Western Boundary Current in the tropical North Atlantic Ocean. *Deep-Sea Research,* **39,** 1967-1984.

OCHOA, J., and N. A. BRAY (1991) Water mass exchange in the Gulf of Cadiz. *Deep-Sea Research,* **38,** 5465-5503.

ORTEGA, G. F. (1972) Isanosteric analysis of the Eastern Caribbean waters during winter. *Boletin Instituto Oceanográfica Universidad de Oriente, Cumara, Venezuela,* **11,** 19-34.

PICKART, R. S., and W. M. SMETHIE, Jr. (in press) How does the deep western boundary current cross the Gulf Stream? *Journal of Physical Oceanography.*

REID, J. L. (1979) On the contribution of the Mediterranean Sea outflow to the Norwegian - Greenland Sea. *Deep-Sea Research,* **26,** 1199-1223.

REID, J. L. (1981) On the mid-depth circulation of the world ocean. In: *Evolution of Physical Oceanography,* B. A. Warren and C. Wunsch, editors, The MIT press, Cambridge, MA and London, England, 70-111.

REID, J. L. (1986) On the total geostrophic circulation of the South Pacific Ocean: Flow patterns, tracers and transports. *Progress in Oceanography,* **16,** 1-61.

REID, J. L. (1989) On the total geostrophic circulation of the South Atlantic Ocean: Flow patterns, tracers and transports. *Progress in Oceanography,* **23,** 149-244.

REID, J. L. (1991) A preliminary study of the mid-depth circulation of the North Atlantic Ocean. *International Association of the Physical Sciences of the Oceans of the International Union of Geodesy and Geopysics. IAPSO Proceedings XX General Assembly.* Vienna, Austria, August 1991. IAPSO Proceedings Number 18, p113.

REID, J. L., and R. J. LYNN (1971) On the influence of the Norwegian - Greenland and Weddell seas upon the bottom waters of the Indian and Pacific oceans. *Deep-Sea Research,* **18,** 1063-1088.

REID, J. L., and A. W. MANTYLA (1989) Circumpolar water in the North Atlantic Ocean. *EOS,* **70,** 1132.

REID, J. L., W. D. NOWLIN, JR., and W. C. PATZERT (1977) On the characteristics and circulation of the southwestern Atlantic Ocean. *Journal of Physical Oceanography,* 7(1), 62-91.

RICHARDSON, P. L. (1977) On the crossover between the Gulf Stream and the Western Boundary Undercurrent. *Deep-Sea Research,* **24,** 139-159.

RICHARDSON, P. L. and T. McKEE (1984) Average seasonal variation of the Atlantic equatorial currents from historical ship drifts. *Journal of Physical Oceanography,* **14,** 1226-1238.

RINTOUL, S. R. (1988) Mass, heat and nutrient fluxes in the Atlantic Ocean determined by inverse methods. *Ph.D. thesis, MIT/WHOI Joint Program in Oceanography,* 287 pp.

RINTOUL, S. R., and C. WUNSCH (1991) Mass, heat, oxygen and nutrient fluxes in the North Atlantic Ocean. *Deep-Sea Research,* **38,** 5355-5378.

ROEMMICH, D. (1981) Circulation of the Caribbean Sea: A well-resolved inverse problem. *Journal of Geophysical Research,* **86,** 7993-8005.

ROEMMICH, D., and C. WUNSCH (1985) Two transatlantic sections: meridional circulation and heat flux in the subtropical North Atlantic Ocean. *Deep-Sea Research,* **32,** 619-664.

SAUNDERS, P. M. (1982) Circulation in the eastern North Atlantic. *Journal of Marine Research,* **40,** 641-657.

SAUNDERS, P. M. (1987) Flow through Discovery Gap. *Journal of Physical Oceanography,* **17,** 631-643.

SCHMITZ, W. J., Jr., and P. L. RICHARDSON (1991) On the sources of the Florida Current. *Deep-Sea Research*, **38**, S379-S409.

SCHOPP, R., and M. ARHAN (1986) A ventilated mid-depth circulation model for the eastern North Atlantic. *Journal of Physical Oceanography*, **16**, 344-357.

SIEVERS, H. A., and W. D. NOWLIN, Jr. (1984) The stratification and water masses at Drake Passage. *Journal of Geophysical Research*, **89**, 10, 489-510, 514.

SPEER, K. G., and M. S. McCARTNEY (1991) Tracing lower North Atlantic deep water across the equator. *Journal of Geophysical Research*, **96**, 20,443-20,448.

STEELE, J. H., J. R. BARRETT, and L. V. WORTHINGTON (1962) Deep currents south of Iceland. *Deep-Sea Research*, **9**, 465-474.

STEFANSSON, U. (1962) North Icelandic waters. *Rit Fiskideild.*, **3**, 269 pp.

SWALLOW, J. C., W. J. GOULD, and P. M. SAUNDERS (1977) Evidence for a poleward eastern boundary current in the North Atlantic Ocean. *International Council for the Exploration of the Sea CM 1977*, **C:32**, Hydrography Committee.

SWALLOW, J. C., and L. V. WORTHINGTON (1961) An observation of a deep counter- current in the western North Atlantic. *Deep-Sea Research*, **8**, 1-19.

SWIFT, J. H. (1984) The circulation of the Denmark Strait and Iceland - Scotland overflow waters in the North Atlantic. *Deep-Sea Research*, **31**, 1339-1355.

SWIFT, J. H., K. AAGAARD, and S. A. MALMBERG (1980) The contribution of the Denmark Strait overflow to the deep North Atlantic. *Deep-Sea Research*, **27A**, 29-42.

TAIT, J. B., A. J. LEE, U. STEFANSSON, and F. HERMAN (1967) Temperature and salinity distributions and water masses of the region. In: *The Iceland - Faeroe Ridge International (ICES) "Overflow" Expedition, May-June, 1960. An investigation of cold, deep water overspill into the northeastern Atlantic Ocean*, J. B. Tait, editor, *Rapports et Procés Verbaux des Reunions Extrait du Journal du Conseil International pour l'Exploration de la Mer*, **157**, 38-149.

TALLEY, L. D., and M. S. McCARTNEY (1982) Distribution and circulation of Labrador Sea water. *Journal of Physical Oceanography*, **12**, 1189-1205.

TSUCHIYA, M. (1985) Evidence of a double-cell subtropical gyre in the South Atlantic Ocean. *Journal of Marine Research*, **43**, 57-65.

TSUCHIYA, M. (1986) Thermostads and circulation in the upper layer of the Atlantic Ocean. *Progress in Oceanography*, **16**, 235-267.

TSUCHIYA, M. (1989) Circulation of the Antarctic Intermediate Water in the North Atlantic Ocean. *Journal of Marine Research*, **47**, 747-755.

TSUCHIYA, M., L. D. TALLEY, and M. S. McCARTNEY (1992) An eastern Atlantic section from Iceland southward across the equator. *Deep-Sea Research*, **39**, 1885-1918.

WARREN, B. A. (1981) Deep circulation of the world ocean. In: *Evolution of physical oceanography*, Bruce A. Warren and Carl Wunsch, editors, The MIT Press, Cambridge, MA, and London, England, pp. 6-41.

WEISS, R. F., J. L. BULLISTER, R. H. GAMMON, and M. J. WARNER (1985) Atmospheric chlorofluoromethanes in the deep equatorial Atlantic. *Nature*, **314**(6012), 608-610.

WHITWORTH, T., III, W. D. NOWLIN, Jr., and S. J. WORLEY (1982) The net transport of the Antarctic Circumpolar Current through Drake Passage. *Journal of Physical Oceanography*, **12**, 960-971.

WORTHINGTON, L. V. (1970) The Norwegian Sea as a Mediterranean basin. *Deep-Sea Research*, **17**, 77-84.

WORTHINGTON, L. V. (1976) On the North Atlantic circulation. *Johns Hopkins Oceanographic Studies*, **6**, 110 pp.

WORTHINGTON, L. V., and G. H. VOLKMANN (1965) The volume transport of the Norwegian Sea overflow water in the North Atlantic. *Deep-Sea Research*, **12**, 667-676.

WORTHINGTON, L. V., and W. R. WRIGHT (1970) North Atlantic Ocean Atlas of potential temperature and salinity in the deep water including temperature, salinity and oxygen profiles from the Erika Dan cruise of 1962. *Woods Hole Oceanographic Institution Atlas Series 2:* 24 pp. and 58 plates.

WÜST, G. (1935) Schichtung und Zirkulation des Atlantischen Ozeans. Die Stratosphäre. In *Wissenschaftliche Ergebnisse der Deutschen Atlantischen Expedition auf dem Forschungs — und Vermessungsschiff "Meteor" 1925-1927*, **6** 1st Part, 2, 109-288.

WÜST, G., and A. DEFANT (1936) Atlas zur Schichtung und Zirkulation des Atlantischen Ozeans. Schnitte und Karten von Temperatur, Salzgehalt und Dichte. In *Wissenschaftliche Ergebnisse der Deutschen Atlantischen Expedition auf dem Forschungs — und Vermessungsschiff "Meteor" 1925-1927*, **6** Atlas, 103 plates.

TABLE 1. EXPEDITIONS FROM WHICH STATIONS WERE CHOSEN TO CALCULATE THE ADJUSTED STERIC HEIGHT.

Expedition/Ship	Dates	NODC #	Source
AJAX Leg 1	Oct.-Nov. 1983	318628	SIO, TAMU (1985)
Atlantis I Cr. 212	Dec. 1954	313281	WHOI
Atlantis II Cr. 9	Jan.-Feb. 1964	310251	WHOI
Atlantis II Cr. 109	June-Sept. 1981	318811	WHOI
Chain Cr. 11	Jan.-Feb. 1960	310271	WHOI
Chain Cr. 12	Apr.-June 1960	313270	WHOI
Crawford Cr. 10	Feb.-May 1957	310583	WHOI
Crawford Cr. 16	Oct.-Dec. 1957	310623	WHOI
Crawford Cr. 17	Feb. 1958	310816	WHOI
Crawford Cr. 40	Apr.-June 1960	313269	WHOI
Crawford Cr. 91	Feb.-Apr. 1963	310993	WHOI
Discovery II Cr. 1	Apr.-Dec. 1957	740622	IGY
Discovery II Cr. 3	Aug.-Sept. 1958	740596	IGY
Erica Dan	Jan.-Apr. 1962	310170	WHOI
Endeavor Cr. 129	Apr. 1985	323074	WHOI
Hildago Cr. 126	Feb.-Mar. 1962	310085	TAMU
Hudson	Apr. 1966	180098	Bedford
Hudson	Mar. 1967	180396	Bedford
Knorr Cr. 104	July-Aug. 1983	318813	WHOI
Knorr	May 1986	318814	WHOI
Le Suroit	July-Sept. 1983	358399-358400	TOPOGULF Group
Meteor Cr. 56	Mar.-Apr. 1981	06	
Meteor	July-Aug. 1984	06	TOPOGULF Group
Oceanus Cr. 133 Leg 2	Jan. 1983	323075	WHOI
Oceanus Cr. 133 Leg 7	May 1983	328663	WHOI
Poseidon	Sept.-Oct. 1983	06	TOPOGULF Group
SAVE Leg 1	Nov.-Dec. 1987	313522	SIO (1992)
TTO NAS	May-Aug. 1981	318657	SIO (1986)
TTO TAS	Dec. 1982 - Feb. 1983	313188	SIO (1986)

TABLE 2. SPECIFICATIONS OF THE ISOPYCNAL SURFACES.

The potential density is expressed as σ_0 from 0-500 db, as σ_1 from 500-1500 db, as σ_2 from 1500-2500 db, as σ_3 from 2500-3500 db, and as σ_4 from 3500-4500 db, and σ_5 from 4500 db to the bottom. Along the isopycnal defined by 34.64 in $\sigma_{1.5}$, $\sigma_{0.5}$ was used from 250-750 db and $\sigma_{1.5}$ below 1250 db. The potential density is given in units of σ, which is ρ - 1000, where ρ is in kg m^{-3}. This table lists the different numbers used for each isopycnal as it extends to the different pressure ranges. The numbers in bold-face type are those used in the text and figures to identify each isopycnal.

North Atlantic

σ_0	$\sigma_{.5}$	σ_1	$\sigma_{1.5}$	σ_2	σ_3	σ_4	σ_5
26.750		31.090					
27.440		**31.938**					
27.630		**32.200**					
27.777	30.082	32.376	**34.640**				
27.824 27.847*		32.456 32.466*		**36.980**	41.395		
27.846 27.871*		32.485 32.499*		37.017 37.018*	**41.440**		
27.874 27.915*		32.523 32.547*		37.067 37.073*	**41.500**	45.838	
27.892		32.548		37.099 37.105*	41.539	**45.880**	
27.901		32.560		37.115 37.125*	41.562	**45.907**	
27.908		32.569		37.126 37.134*	41.572	**45.920**	50.173

*used east of the Reykjanes Ridge

South Atlantic

σ_0	$\sigma_{.5}$	σ_1	$\sigma_{1.5}$	σ_2	σ_3	σ_4
26.750						
27.300		**31.938** 31.948 60°-90°S				
27.630 27.563 60°-90°S		**32.200**				
27.675	30.035	32.355	**34.640**			
27.775		32.425		**36.980**	41.400	
27.770		32.445		37.013 37.004 30°-90°S	**41.440**	
27.787		32.476		37.041	**41.500**	45.840
27.800 27.764 70°-90°S		32.487		37.057	41.538 41.534 10°-30°S 41.528 30°-40°S 41.521 40°-90°S	**45.880**
27.804		32.498		37.074	41.547	**45.907**
27.815 27.808 60°-70°S 27.785 70°-90°S		32.502		37.080	41.564 41.556 30°-40°S 41.553 40°-90°S	**45.920**

Fig. 1, 2

Fig. 1. Principal topographic features referred to in the text.

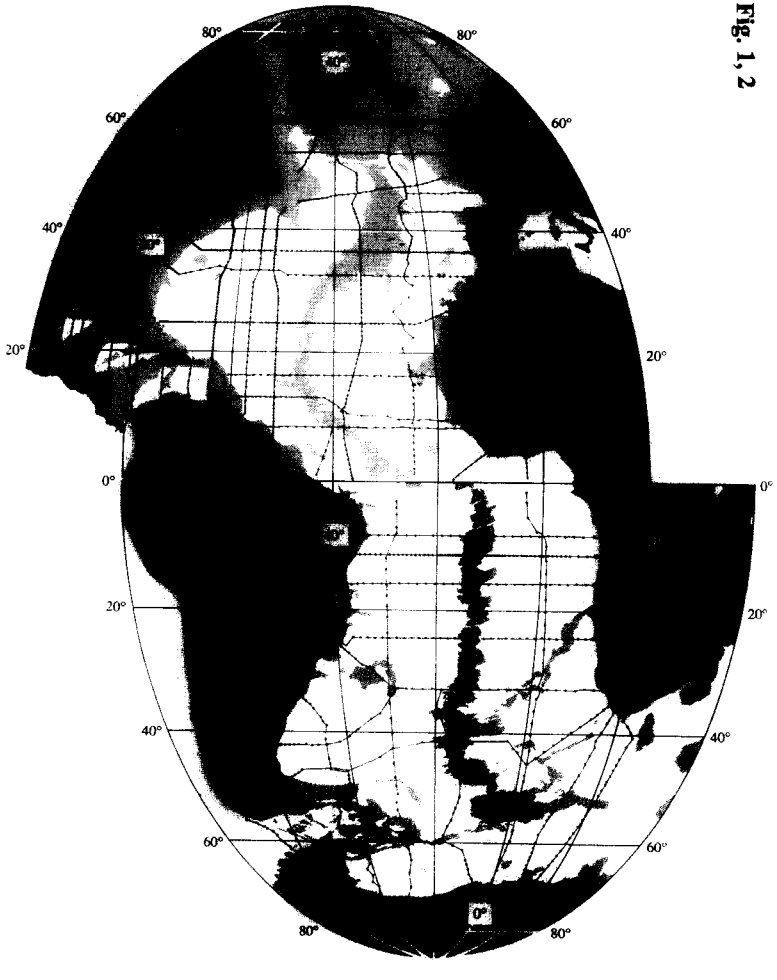

Fig. 2. Lines of stations used in the calculation of the geostrophic flow.

Fig. 3

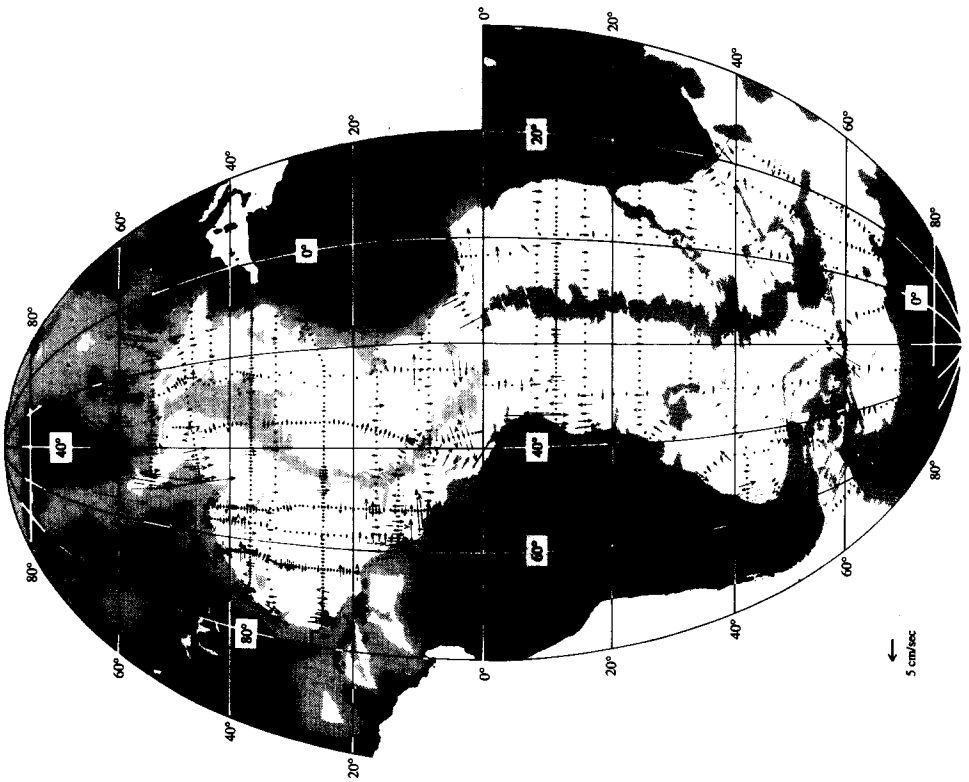

Fig. 3. Bottom velocity for each station pair at depths below 1500m. Depths less than 3500m are shaded.

Fig. 4a, 4b
Θ, S

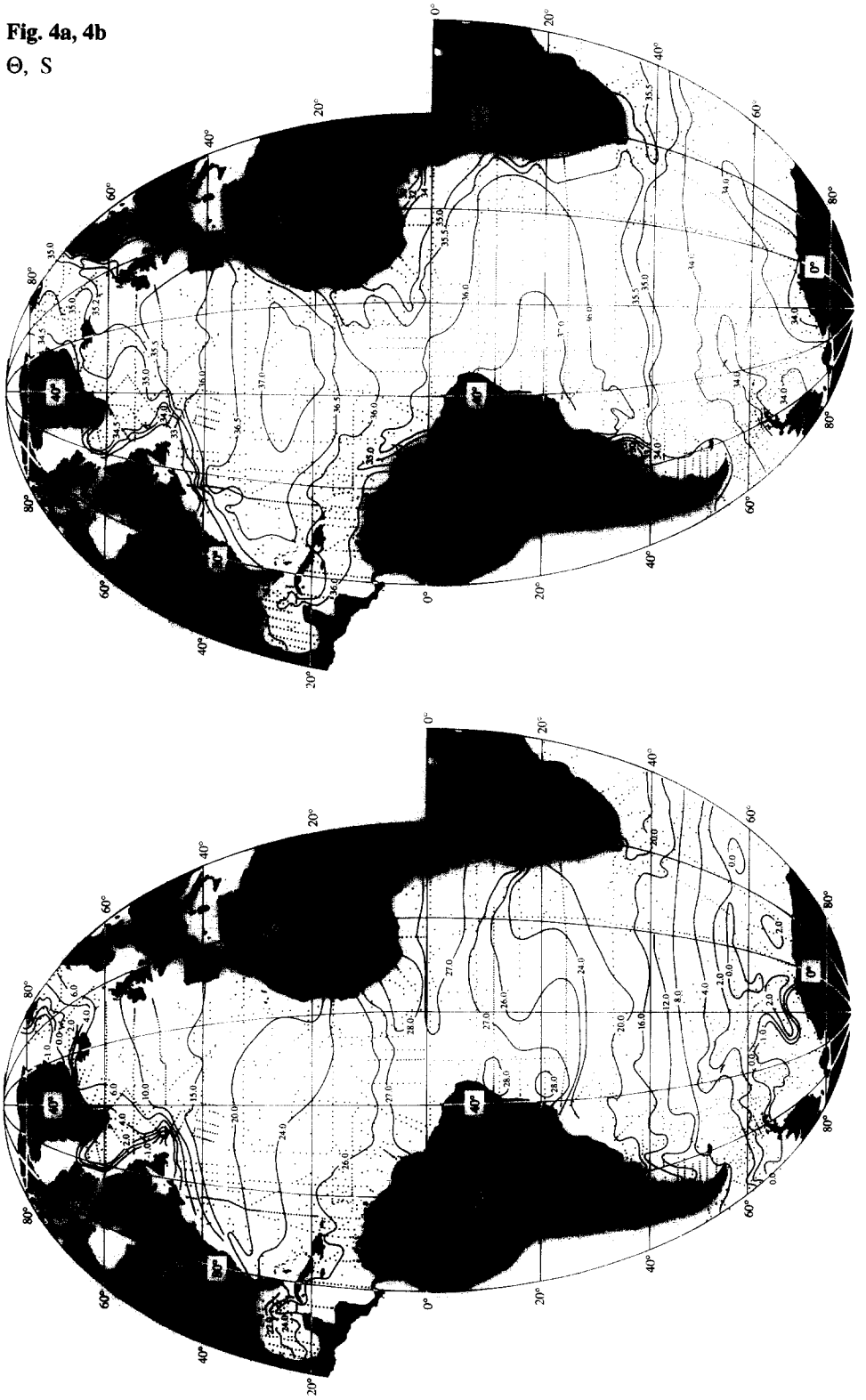

Fig. 4b. Salinity at the sea surface.

Fig. 4a. Temperature (°C) at the sea surface.

Fig. 4c, 4d
σ_0, O_2

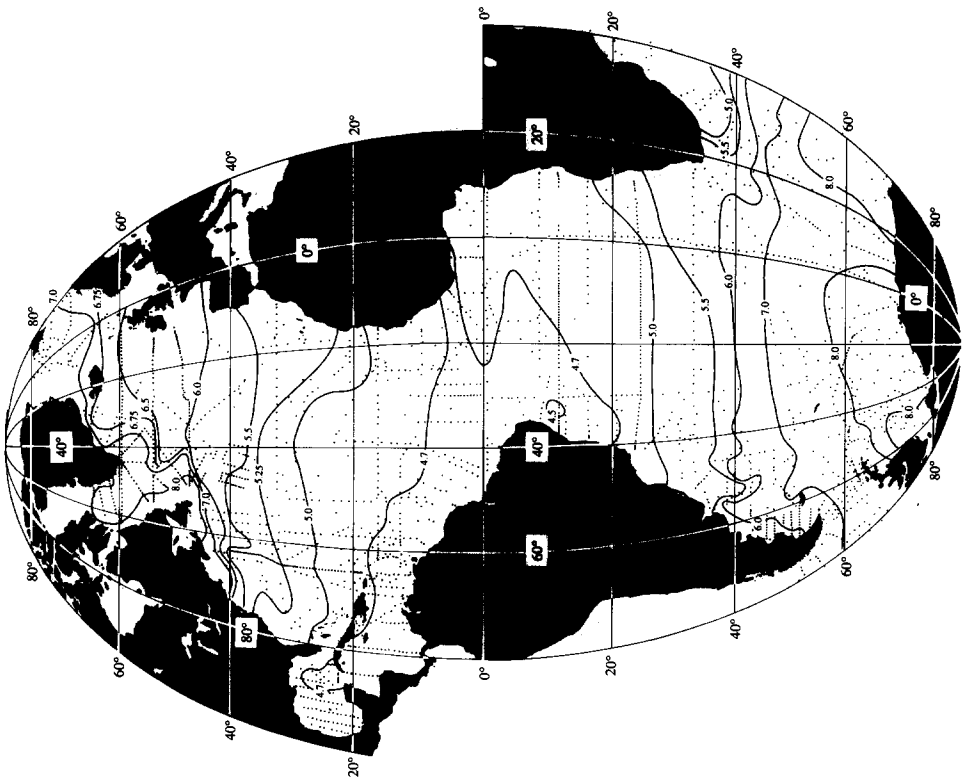

Fig. 4d. Oxygen (ml/l) at the sea surface.

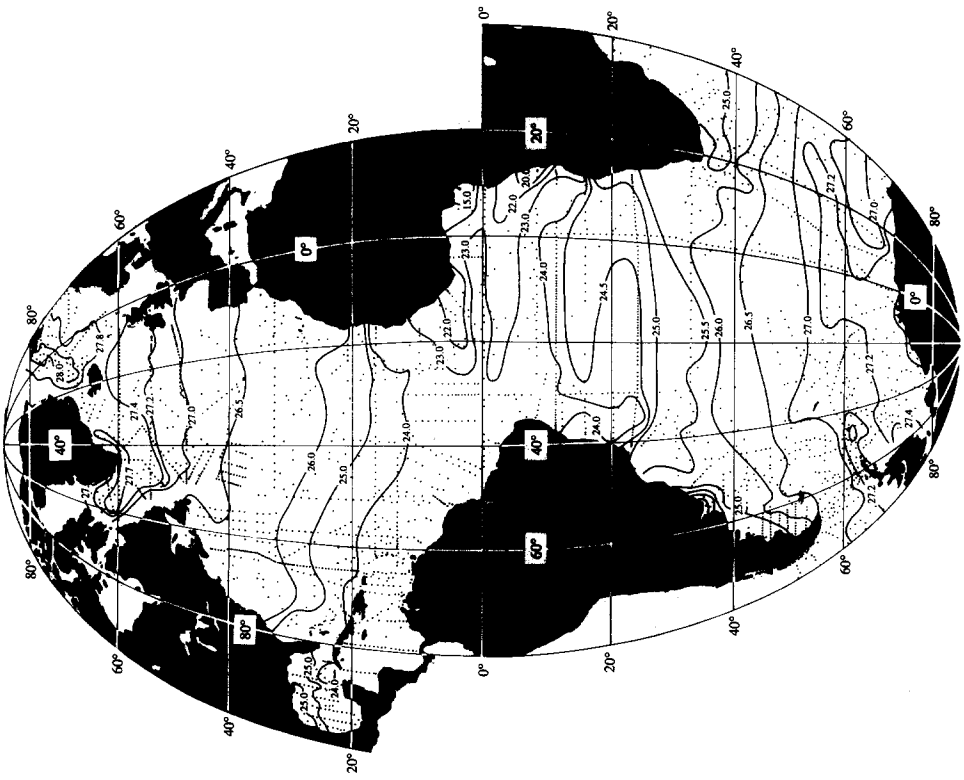

Fig. 4c. Potential density (σ_0) at the sea surface.

Fig. 4e, 4f
NO_3, PO_4

Fig. 4f. Phosphate (μm kg^{-1}) at 100m.

Fig. 4e. Nitrate (μm kg^{-1}) at 100m.

Fig. 4g
SiO_3

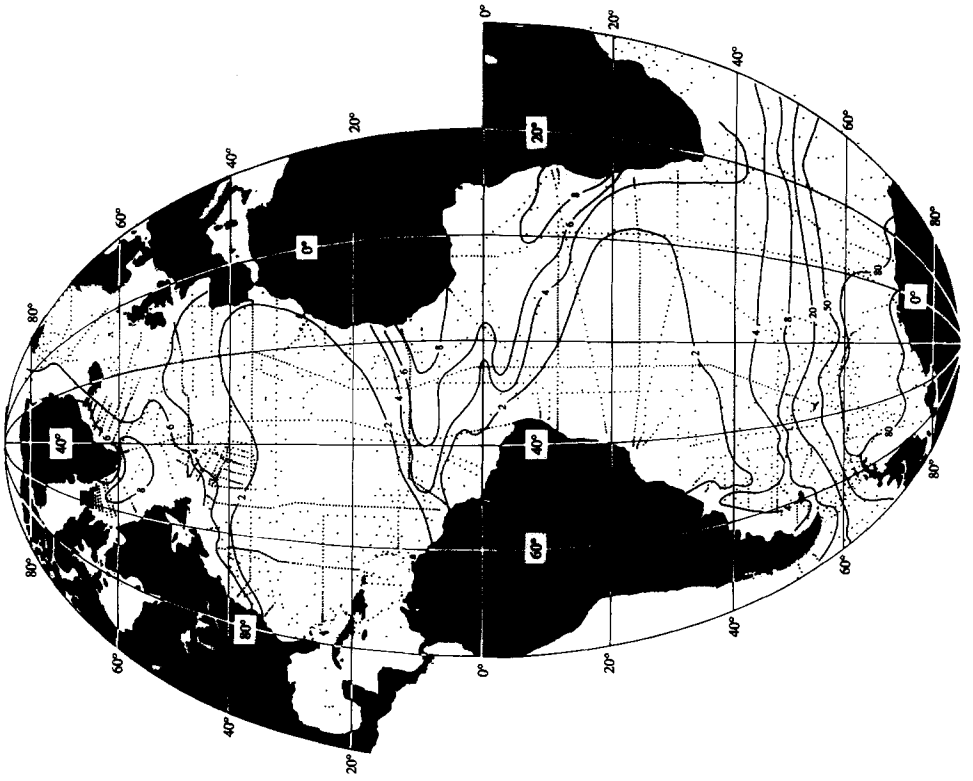

Fig. 4g. Silica (μm kg^{-1}) at 100m.

Fig. 5a, 5b

Θ, S

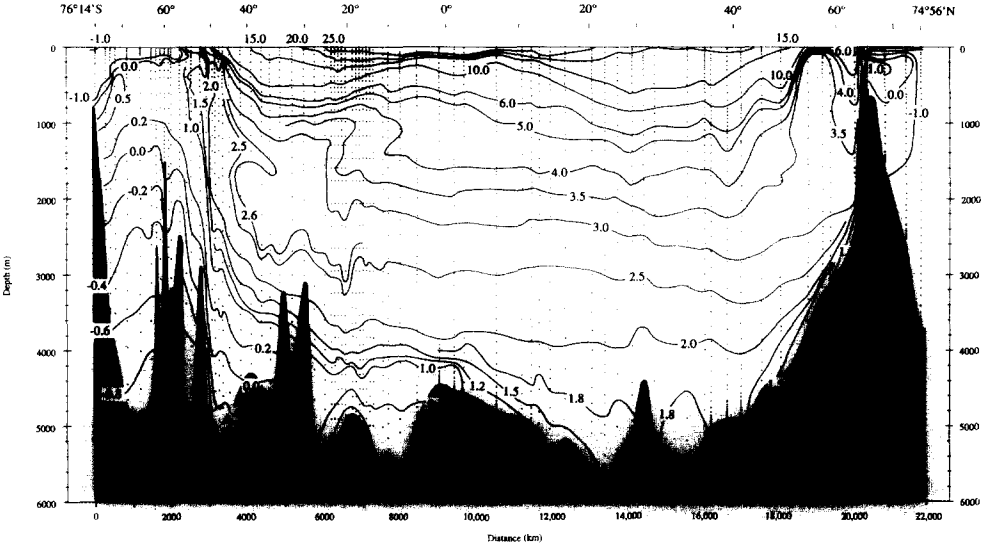

Fig. 5a. Potential temperature (°C) on the north-south section.

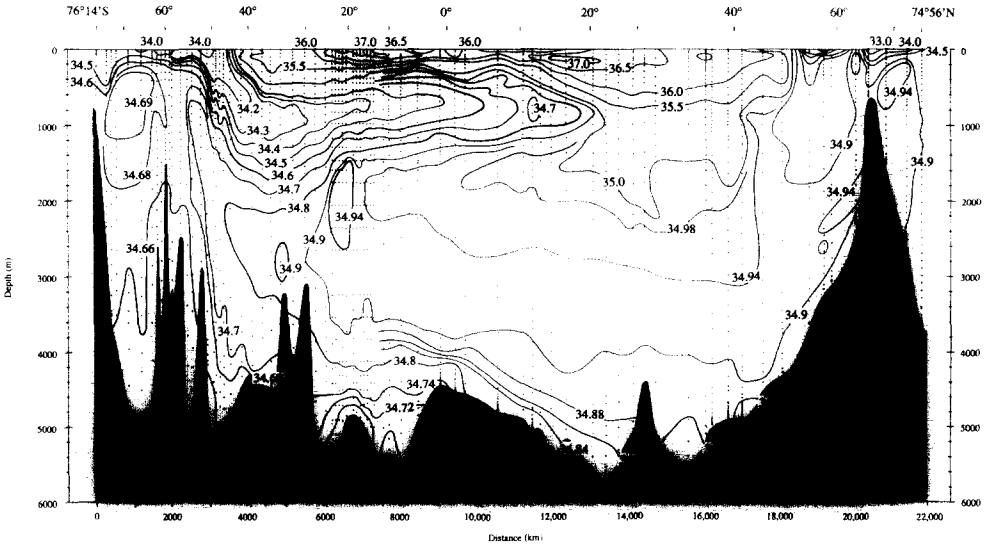

Fig. 5b. Salinity on the north-south section.

Fig. 5c, 5d
$\sigma_0 - \sigma_4$, O_2

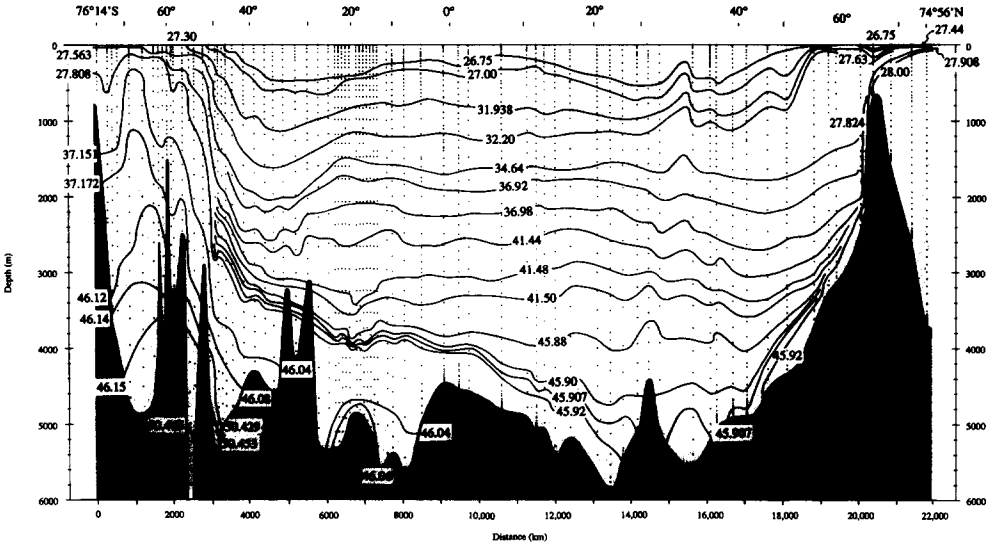

Fig. 5c. Potential density (σ_0 - σ_4) in the north-south section.

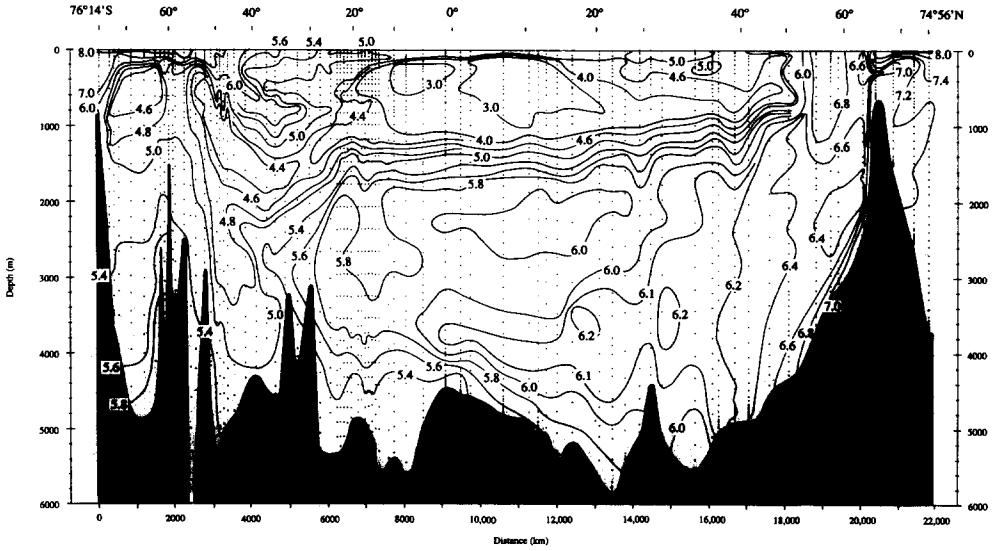

Fig. 5d. Oxygen (ml/l) on the north-south section.

Fig. 5e, 5f
NO_3, PO_4

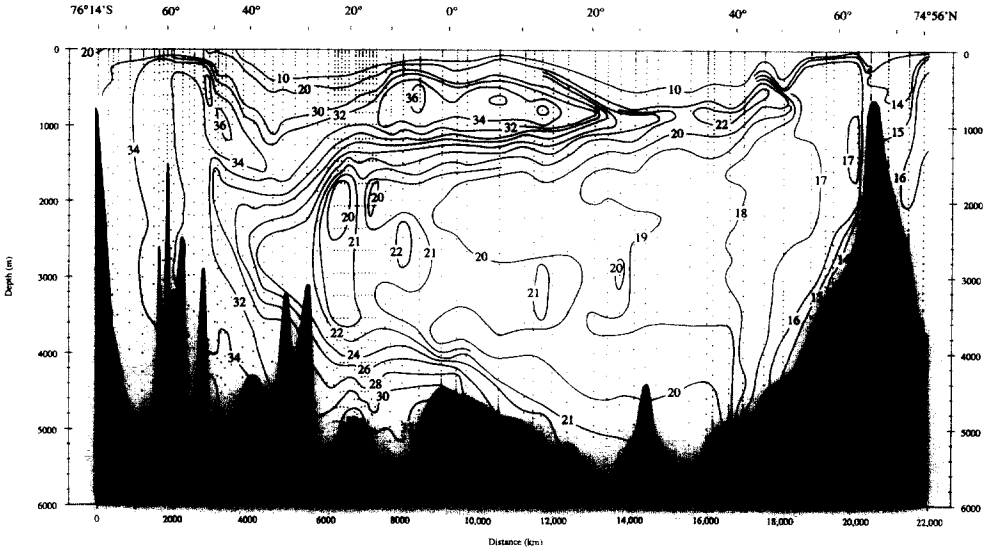

Fig. 5e. Nitrate (μm kg^{-1}) on the north-south section.

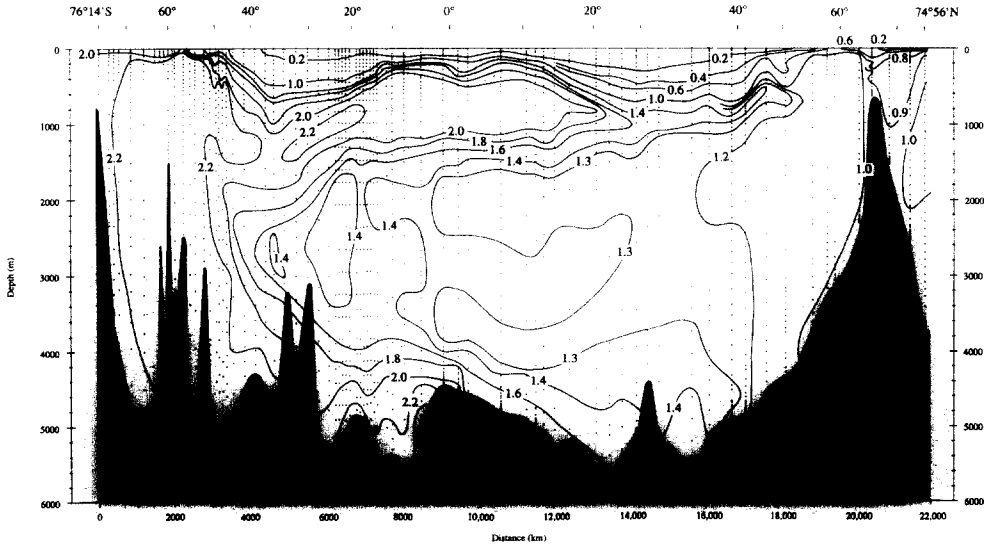

Fig. 5f. Phosphate (μm kg^{-1}) on the north-south section.

Fig. 5g
SiO_3

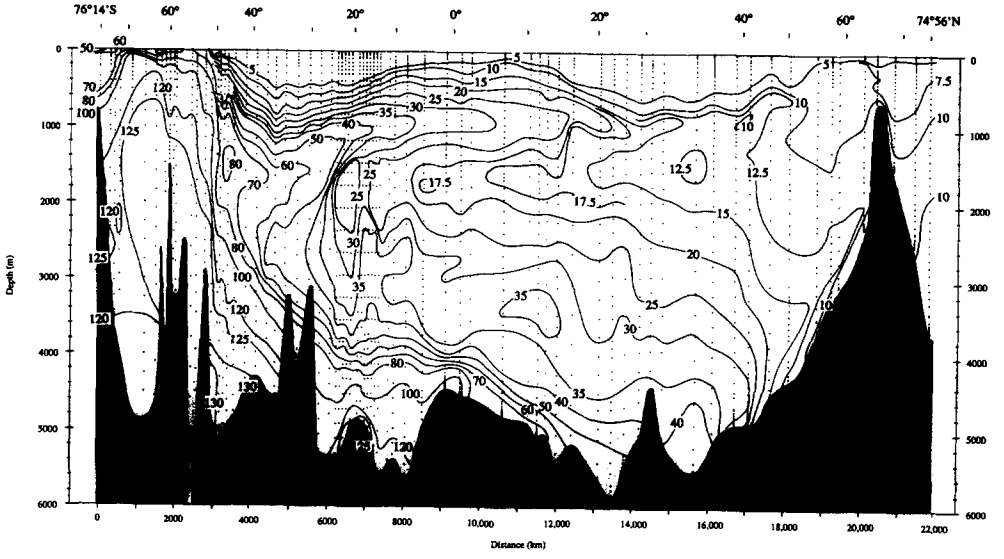

Fig. 5g. Silica (μm kg^{-1}) on the north-south section.

Fig. 6a, 6b
Θ, S

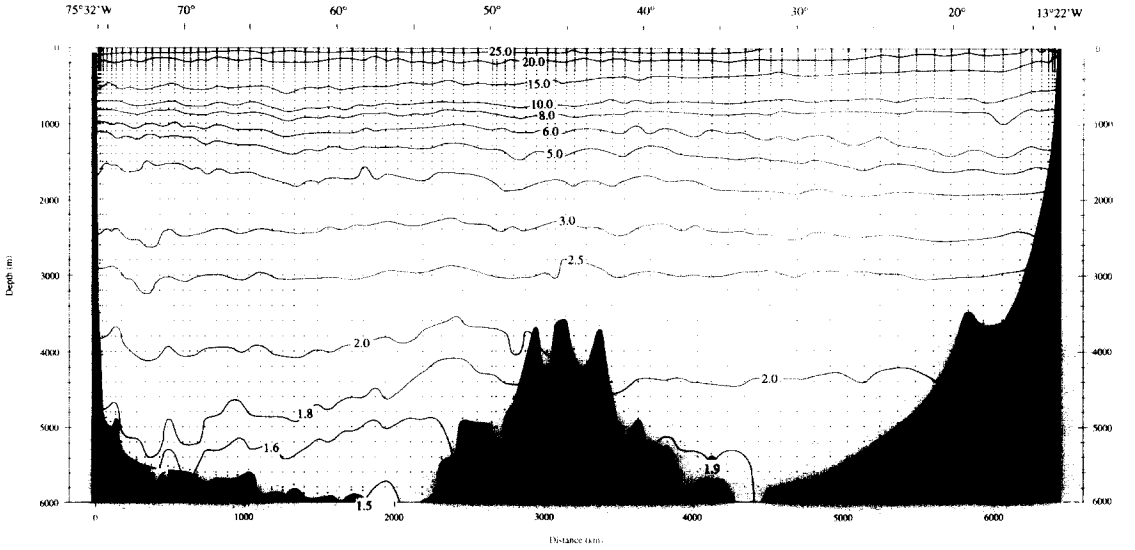

Fig. 6a. Potential temperature (°C) on the section along 24°N.

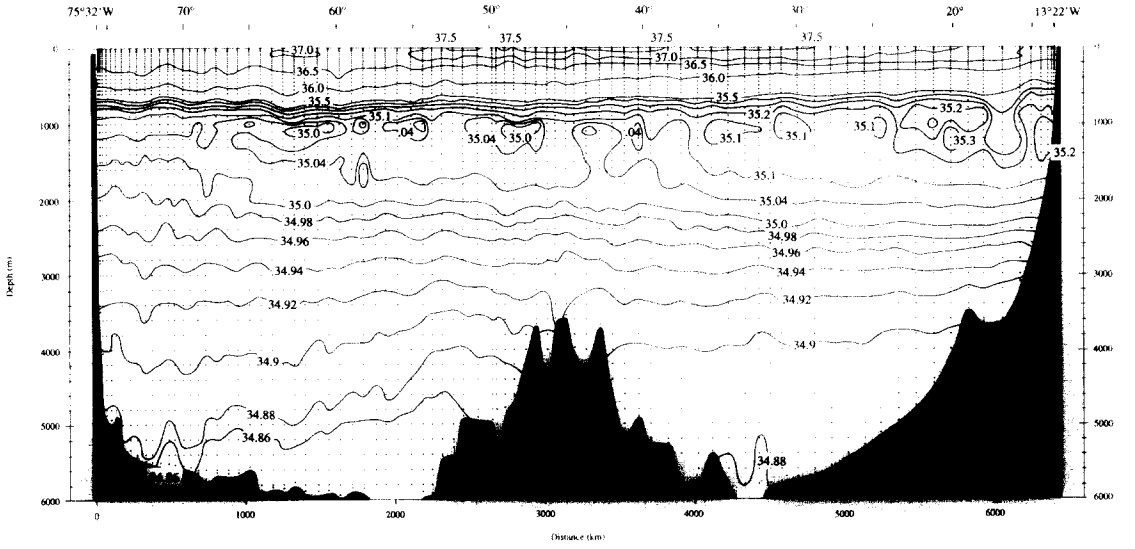

Fig. 6b. Salinity on the section along 24°N.

Fig. 6c, 6d
$\sigma_0 - \sigma_4$, O_2

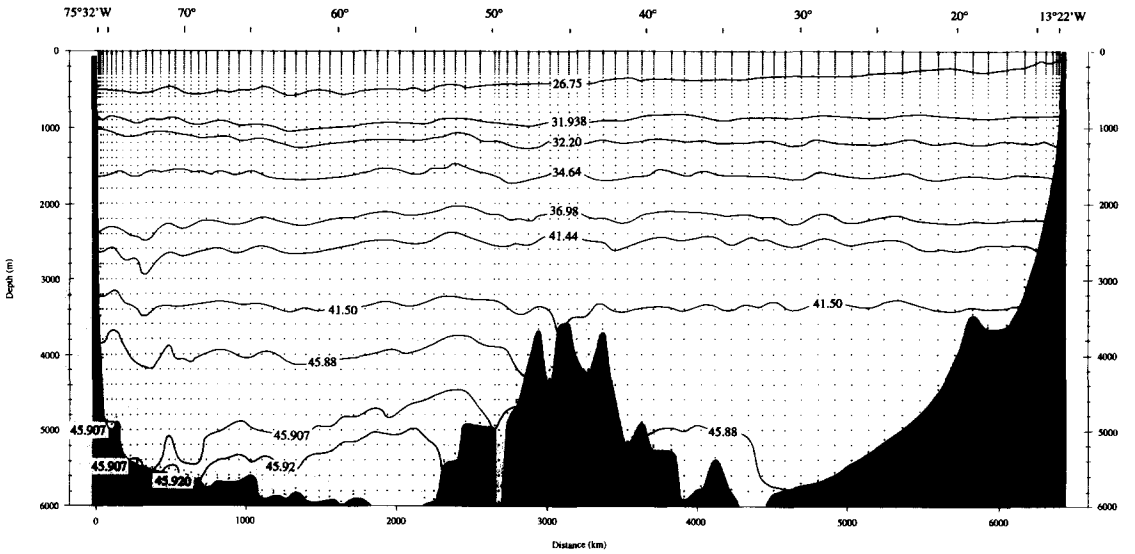

Fig. 6c. Potential density (σ_0 - σ_4) on the section along 24°N.

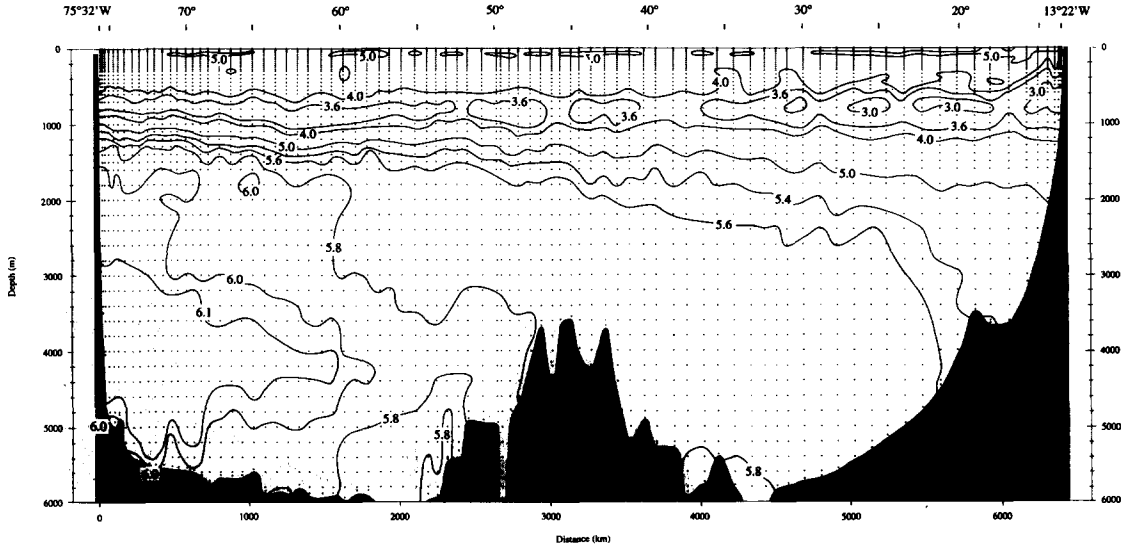

Fig. 6d. Oxygen (ml/l) on the section along 24°N.

Fig. 6e, 6f
O_2 sat., NO_3

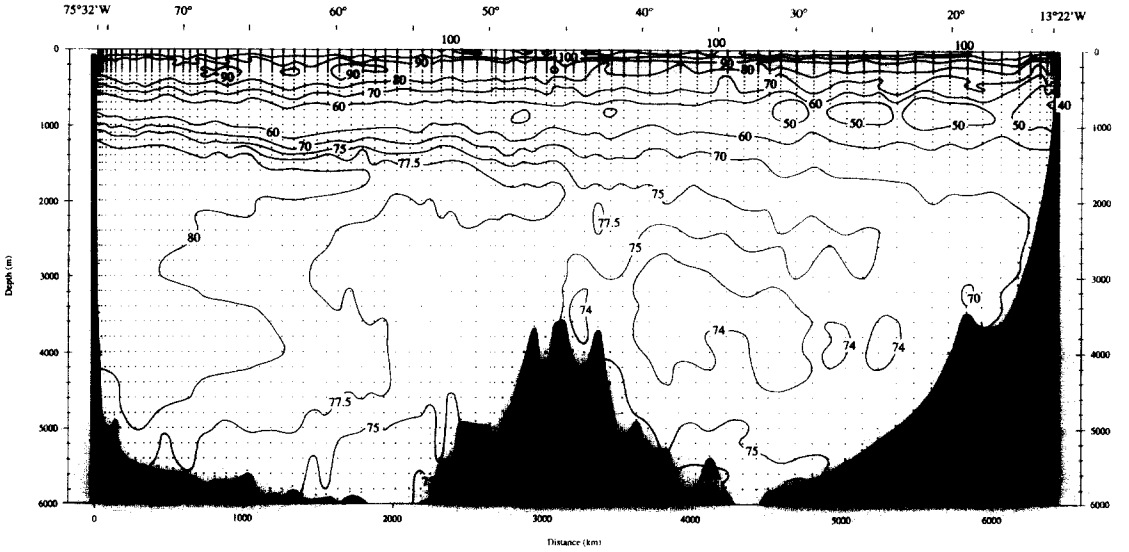

Fig. 6e. Oxygen saturation (%) on the section along 24°N.

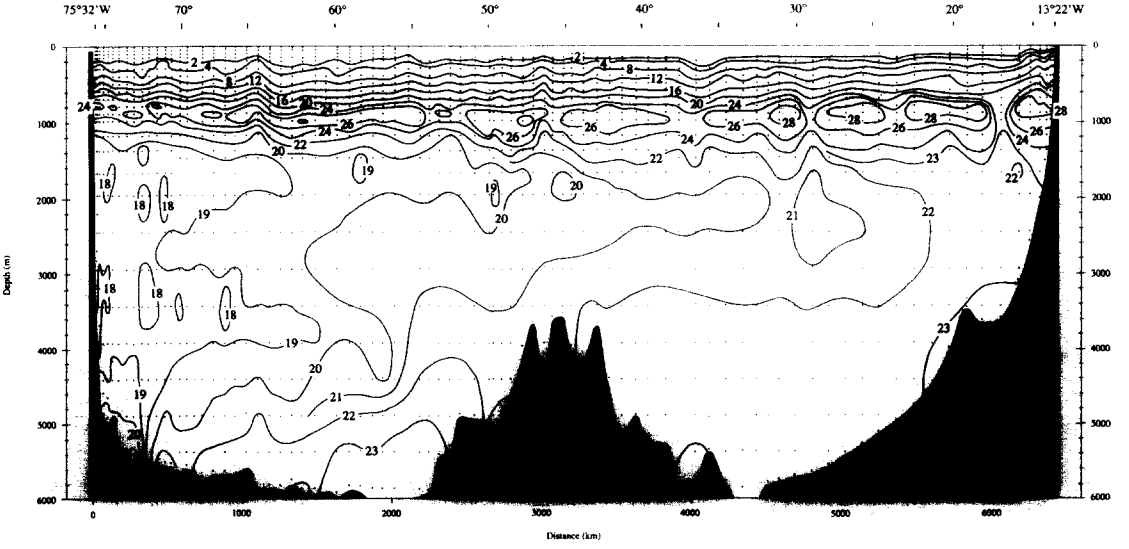

Fig. 6f. Nitrate (μm kg^{-1}) on the section along 24°N.

Fig. 6g, 6h
PO_4, SiO_3

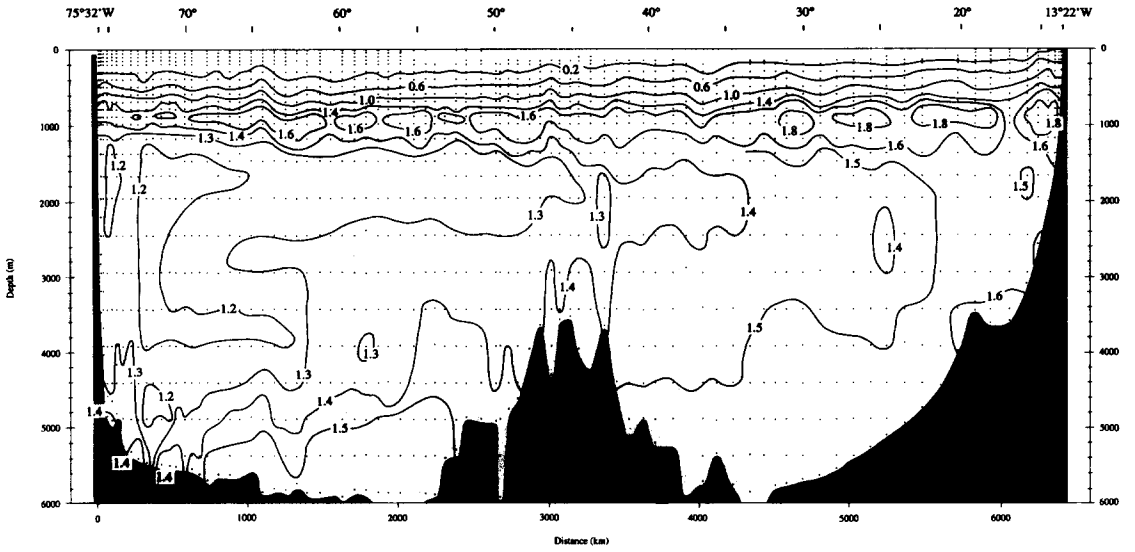

Fig. 6g. Phosphate (μm kg^{-1}) on the section along 24°N.

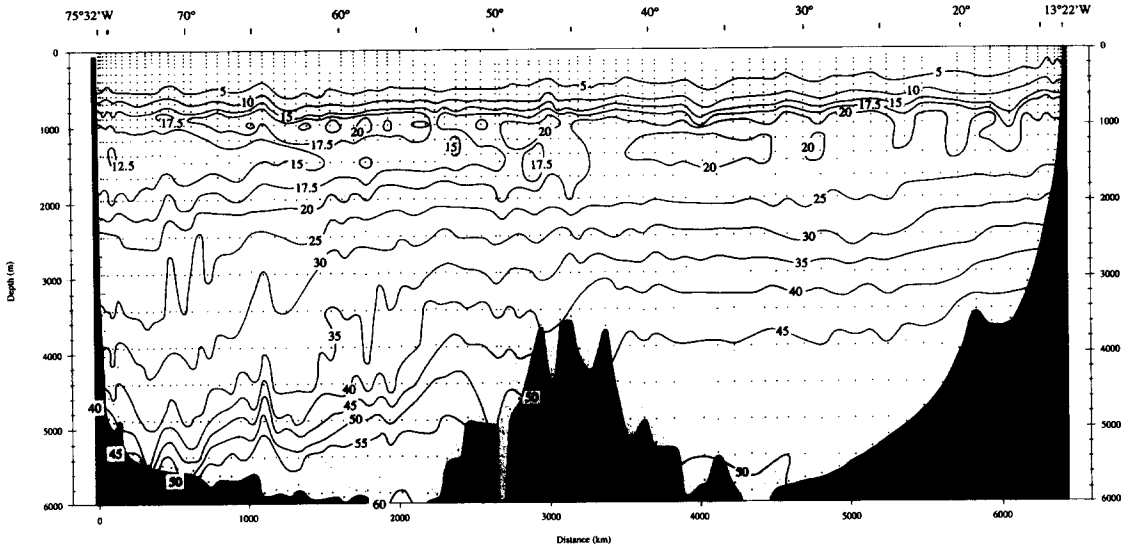

Fig. 6h. Silica (μm kg^{-1}) on the section along 24°N.

Fig. 7a, 7b
Θ, S

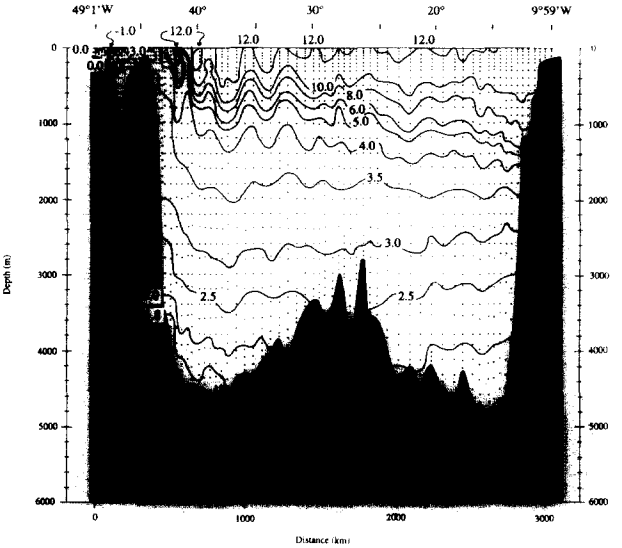

Fig. 7a. Potential temperature (° C) on the section along 47°N

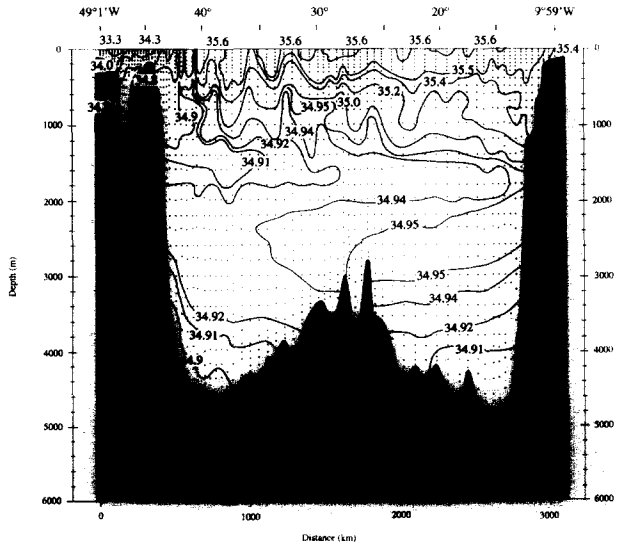

Fig. 7b. Salinity on the section along 47°N.

Fig. 7c, 7d
$\sigma_0 - \sigma_4$, O_2

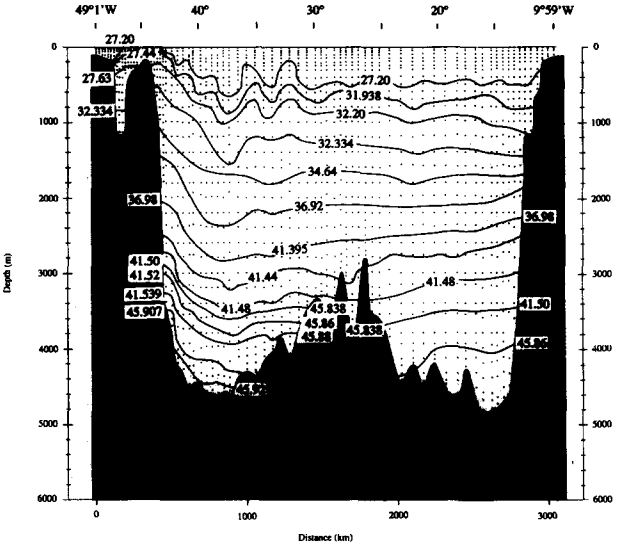

Fig. 7c. Potential density (σ_0 - σ_4) on the section along 47°N.

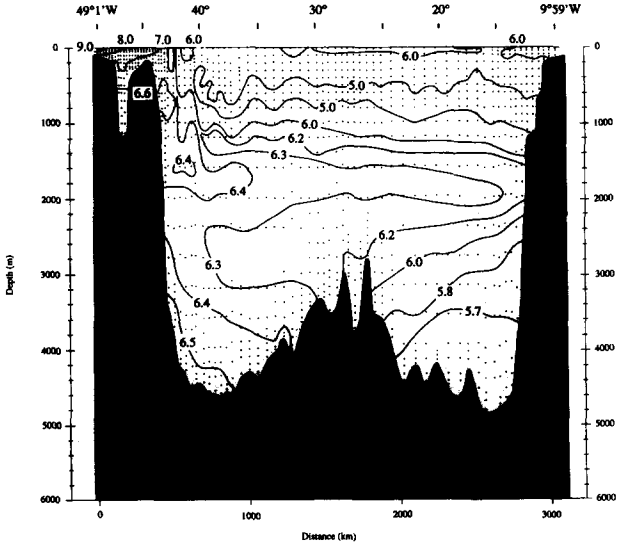

Fig. 7d. Oxygen (ml/l) on the section along 47°N.

Fig. 7e, 7f
NO_3, SiO_3

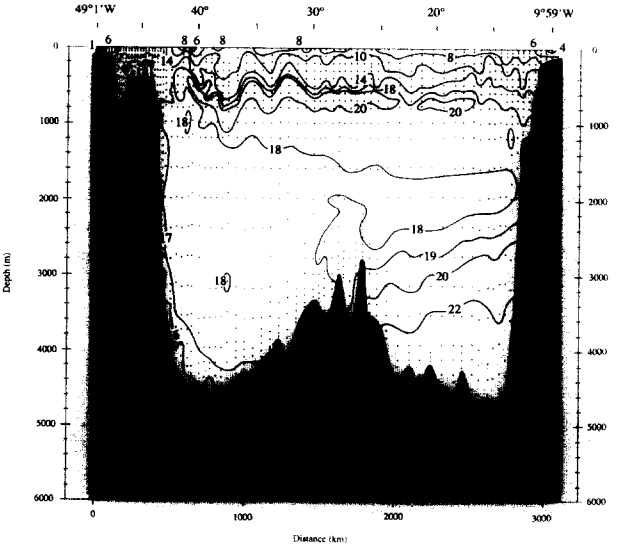

Fig. 7e. Nitrate (μm kg^{-1}) on the section along 47°N.

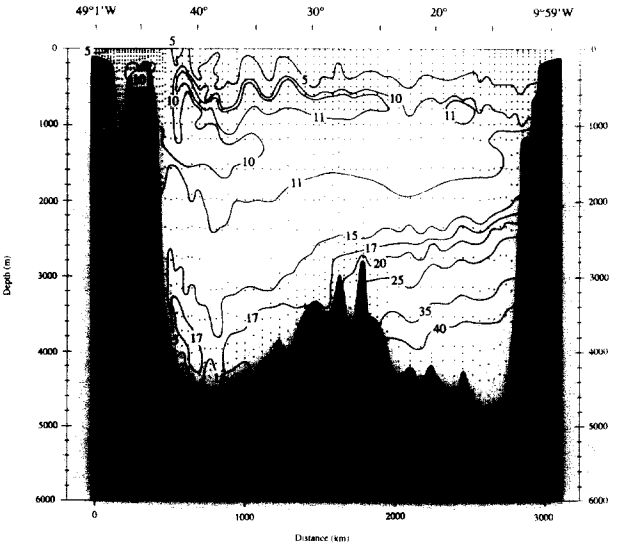

Fig. 7f. Silica (μm kg^{-1}) on the section along 47°N.

Fig. 8a, 8b
Flow 0 db, 250 db

Fig. 8a. Adjusted steric height at 0 db (10 $m^2 s^{-2}$ or 10Jkg^{-1}).

Fig. 8b. Adjusted steric height at 250 db (10 $m^2 s^{-2}$ or 10Jkg^{-1}).

Fig. 8c, 8d
Flow 500 db, 800 db

Fig. 8d. Adjusted steric height at 800 db (10 $m^2 s^{-2}$ or 10Jkg^{-1}).

Fig. 8c. Adjusted steric height at 500 db (10 $m^2 s^{-2}$ or 10Jkg^{-1}).

Fig. 8e, 8f
Flow 1000 db, 1500 db

Fig. 8f. Adjusted steric height at 1500 db ($10\ m^2 s^{-2}$ or $10 J kg^{-1}$).

Fig. 8e. Adjusted steric height at 1000 db ($10\ m^2 s^{-2}$ or $10 J kg^{-1}$).

Fig. 8g, 8h
Flow 2000 db, 2500 db

Fig. 8g. Adjusted steric height at 2000 db (10 $m^2 s^{-2}$ or 10Jkg^{-1}).

Fig. 8h. Adjusted steric height at 2500 db (10 $m^2 s^{-2}$ or 10Jkg^{-1}).

Fig. 8i, 8j
Flow 3000 db, 3500 db

Fig. 8j. Adjusted steric height at 3500 db (10 $m^2 s^{-2}$ or 10Jkg^{-1}).

Fig. 8i. Adjusted steric height at 3000 db (10 $m^2 s^{-2}$ or 10Jkg^{-1}).

Fig. 8k. Adjusted steric height at 4000 db (10 $m^2 s^{-2}$ or 10Jkg^{-1}).

Fig. 8k, 8l
Flow 4000 db, 4500 db

Fig. 8l. Adjusted steric height at 4500 db (10 $m^2 s^{-2}$ or 10Jkg^{-1}).

Fig. 8m, 8n
Flow 5000 db, 5200 db

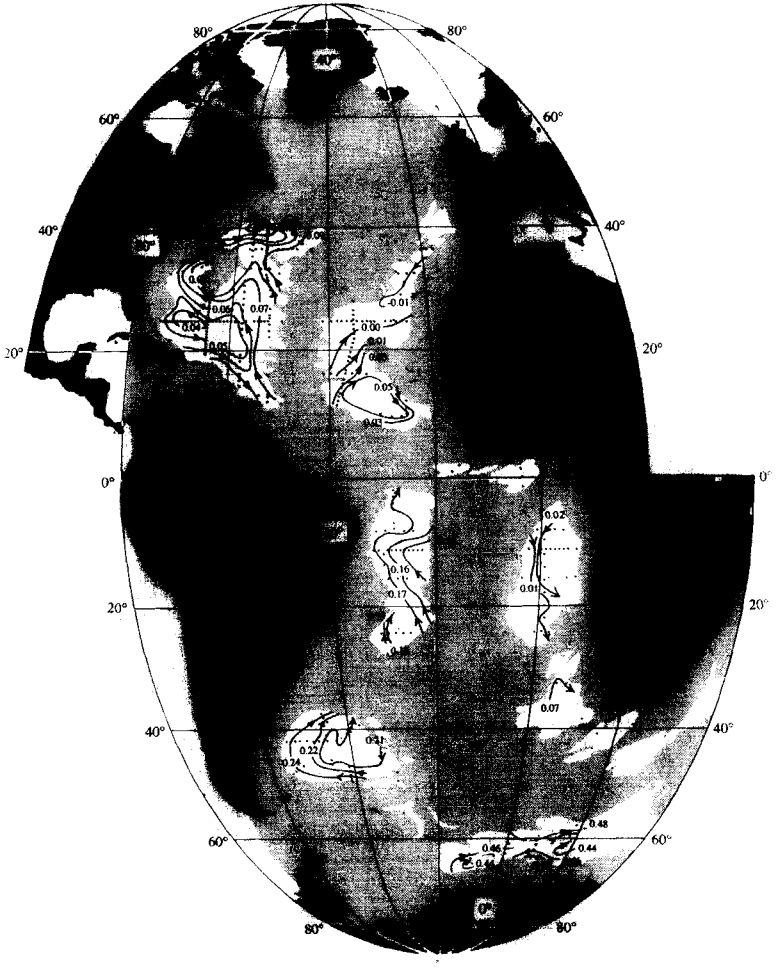

Fig. 8m. Adjusted steric height at 5000 db (10 m^2s^{-2} or 10Jkg^{-1}).

Fig. 8n. Adjusted steric height at 5200 db (10 m^2s^{-2} or 10Jkg^{-1}).

Fig. 8o
Flow at bottom

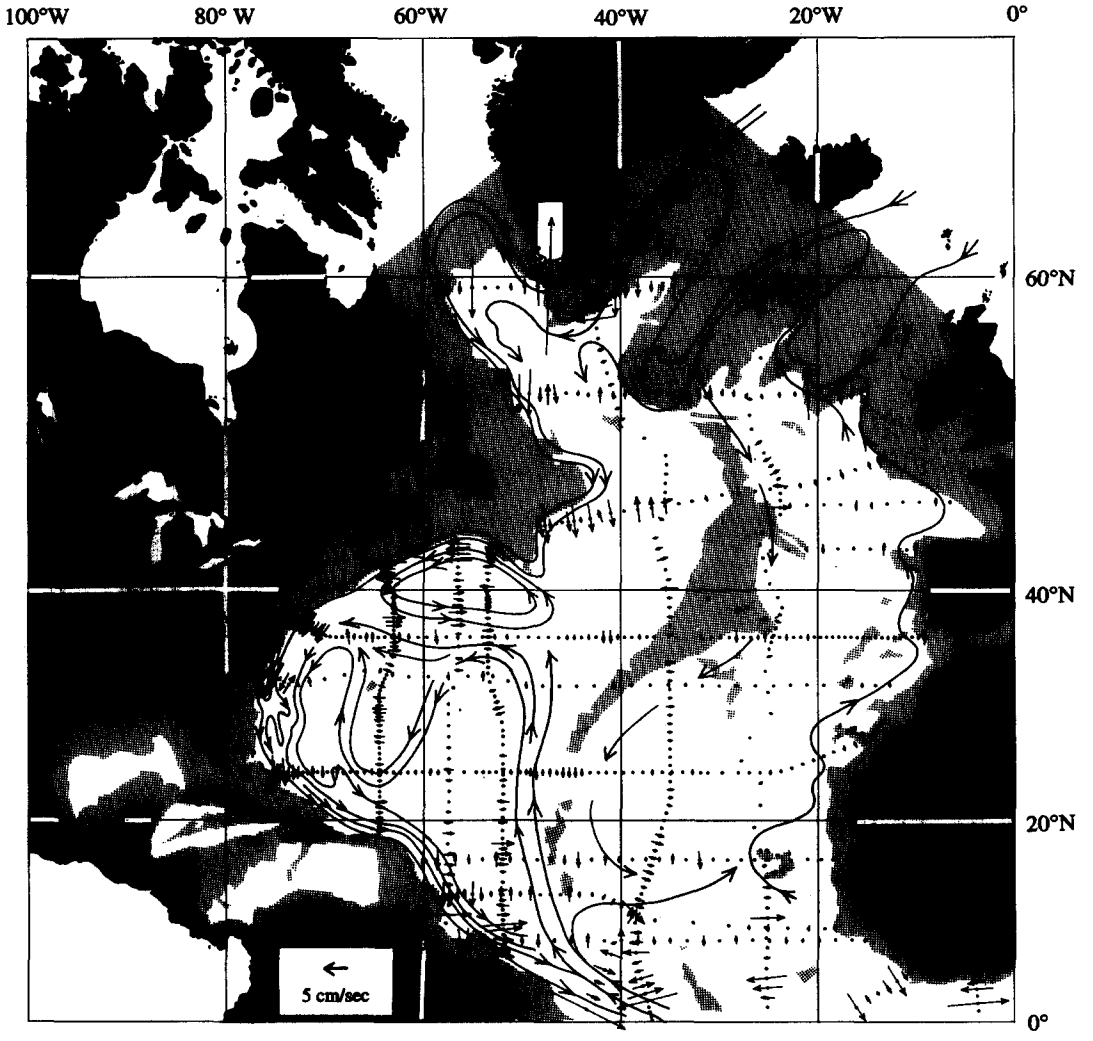

Fig. 8o. The map of deep currents based upon sediment patterns prepared by McCAVE and TUCHOLKE (1986) overlaid on the map of bottom velocities estimated herein at depths greater than 2000 m. The shaded area represents depths less than 3000 m.

Fig. 9
Transport

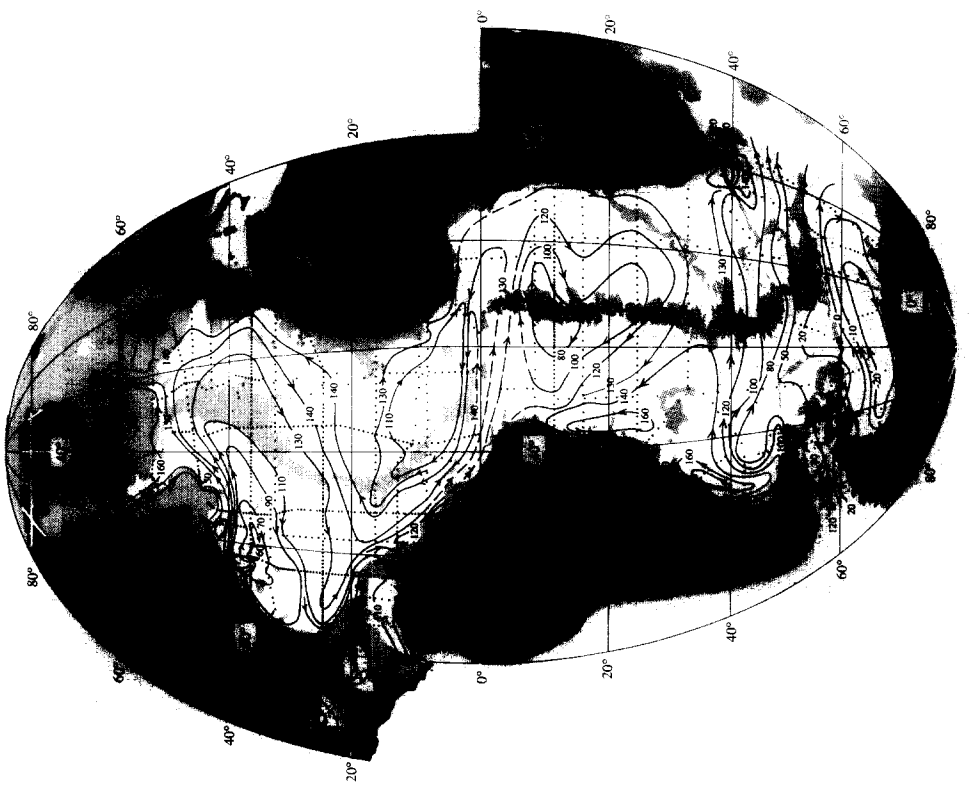

Fig. 9. Transport ($10^6 m^3 s^{-1}$). Integration is from a zero value at the coast of Antarctica and reaches 130 x $10^6 m^3 s^{-1}$ everywhere along the coast of the American continents and Greenland. Along the coasts of Europe and Africa it reaches 132 x $10^6 m^3 s^{-1}$, as 2 x $10^6 m^3 s^{-1}$ are assumed entering the Atlantic across the Greenland-Scotland sills. The shaded area represents depths less than 3500m.

Fig. 10a, 10b
σ_0=26.75 Depth, S

Fig. 10b. Salinity on the isopycnal defined by 26.75 in σ_0.

Fig. 10a. Depth (hm) of the isopycnal defined by 26.75 in σ_0.

Fig. 10c, 10d
σ_0=26.75 O_2, NO_3

Fig. 10c. Oxygen (ml/l) on the isopycnal defined by 26.75 in σ_0.

Fig. 10d. Nitrate (μm kg^{-1}) on the isopycnal defined by 26.75 in σ_0.

Fig. 10e, 10f

σ_0=26.75 PO_4, SiO_3

Fig. 10e. Phosphate (μm kg^{-1}) on the isopycnal defined by 26.75 in σ_0.

Fig. 10f. Silica (μm kg^{-1}) on the isopycnal defined by 26.75 in σ_0.

Fig. 11a, 11b

σ_1=31.938 Depth, S

Fig. 11b. Salinity on the isopycnal defined by 31.938 in σ_1 below 500m.

Fig. 11a. Depth (hm) of the isopycnal defined by 31.938 in σ_1 below 500m.

Fig. 11c, 11d
σ_1=31.938 O_2, NO_3

Fig. 11c. Oxygen (ml/l) on the isopycnal defined by 31.938 in σ_1 below 500m.

Fig. 11d. Nitrate (μm kg^{-1}) on the isopycnal defined by 31.938 in σ_1 below 500m.

Fig. 11e, 11f

σ_1=31.938 PO_4, SiO_3

Fig. 11e. Phosphate (μm kg^{-1}) on the isopycnal defined by 31.938 in σ_1 below 500m.

Fig. 11f. Silica (μm kg^{-1}) on the isopycnal defined by 31.938 in σ_1 below 500m..

Fig. 12a, 12b

σ_1=32.20 Depth, S

Fig. 12a. Depth (hm) of the isopycnal defined by 32.20 in σ_1.

Fig. 12b. Salinity on the isopycnal defined by 32.20 in σ_1.

Fig. 12c, 12d
σ_1=32.20 O_2, NO_3

Fig. 12c. Oxygen (ml/l) on the isopycnal defined by 32.20 in σ_1.

Fig. 12d. Nitrate (μm kg^{-1}) on the isopycnal defined by 32.20 in σ_1.

Fib. 12e, 12f

σ_1=32.20 PO_4, SiO_3

Fig. 12e. Phosphate (μm kg^{-1}) on the isopycnal defined by 32.20 in σ_1.

Fig. 12f. Silica (μm kg^{-1}) on the isopycnal defined by 32.20 in σ_1.

Fig. 13a, 13b

$\sigma_{1.5}$=34.64 Depth, Flow

Fig. 13a. Depth (hm) of the isopycnal defined by 34.64 in $\sigma_{1.5}$.

Fig. 13b. Adjusted steric height along the isopycnal defined by 34.64 in $\sigma_{1.5}$.

Fig. 13c, 13d
$\sigma_{1.5}$=34.64 S, O_2

Fig. 13d. Oxygen (ml/l) on the isopycnal defined by 34.64 in $\sigma_{1.5}$.

Fig. 13c. Salinity on the isopycnal defined by 34.64 in $\sigma_{1.5}$.

Fig. 13e, 13f
$\sigma_{1.5}$=34.64 NO_3, SiO_3

Fig. 13e. Nitrate (μm kg^{-1}) on the isopycnal defined by 34.64 in $\sigma_{1.5}$.

Fig. 13f. Silica (μm kg^{-1}) on the isopycnal defined by 34.64 in $\sigma_{1.5}$.

Fig. 14a, 14b
σ_2=36.98 Depth, S

Fig. 14a. Depth (hm) of the isopycnal defined by 36.98 in σ_2.

Fig. 14b. Salinity on the isopycnal defined by 36.98 in σ_2.

Fig. 14c, 14d
σ_2=36.98 O_2, NO_3

Fig. 14c. Oxygen (ml/l) on the isopycnal defined by 36.98 in σ_2.

Fig. 14d. Nitrate (μm kg^{-1}) on the isopycnal defined by 36.98 in σ_2.

Fig. 14e, 14f
σ_2=36.98 PO_4, SiO_3

Fig. 14e. Phosphate (μm kg^{-1}) on the isopycnal defined by 36.98 in σ_2.

Fig. 14f. Silica (μm kg^{-1}) on the isopycnal defined by 36.98 in σ_2.

Fig. 15a, 15b
σ_3=41.44 Depth, S

Fig. 15b. Salinity on the isopycnal defined by 41.44 in σ_3.

Fig. 15a. Depth (hm) of the isopycnal defined by 41.44 in σ_3.

Fig. 15c, 15d
σ_3=41.44 O_2, PO_4

Fig. 15c. Oxygen (ml/l) on the isopycnal defined by 41.44 in σ_3.

Fig. 15d. Phosphate (μm kg^{-1}) on the isopycnal defined by 41.44 in σ_3.

Fig. 15e
σ_3=41.44 SiO_3

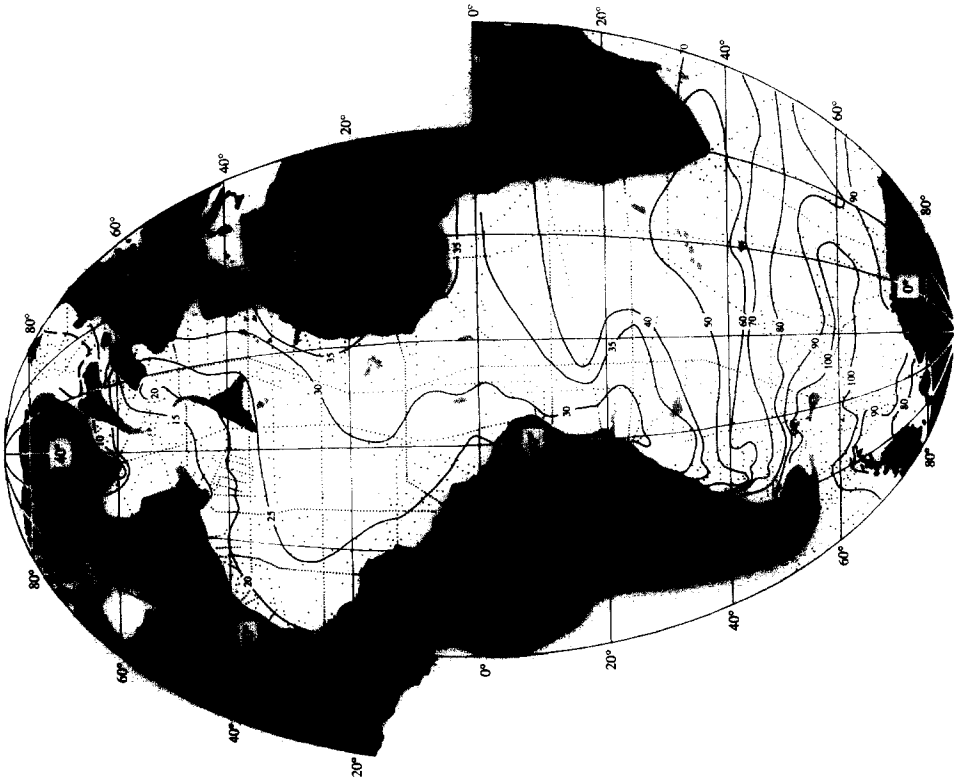

Fig. 15e. Silica (μm kg^{-1}) on the isopycnal defined by 41.44 in σ_3.

Fig. 16a, 16b

σ_3=41.50 Depth, Flow

Fig. 16b. Adjusted steric height along the isopycnal defined by 41.50 in σ_3.

Fig. 16a. Depth (hm) of the isopycnal defined by 41.50 in σ_3.

Fig. 16c, 16d
σ_3=41.50 S, O_2

Fig. 16d. Oxygen (ml/l) on the isopycnal defined by 41.50 in σ_3.

Fig. 16c. Salinity on the isopycnal defined by 41.50 in σ_3.

Fig. 16e, 16f

σ_3=41.50 NO_3, PO_4

Fig. 16e. Nitrate (μm kg^{-1}) on the isopycnal defined by 41.50 in σ_3.

Fig. 16f. Phosphate (μm kg^{-1}) on the isopycnal defined by 41.50 in σ_3.

Fig. 16g
σ_3=41.50 SiO_3

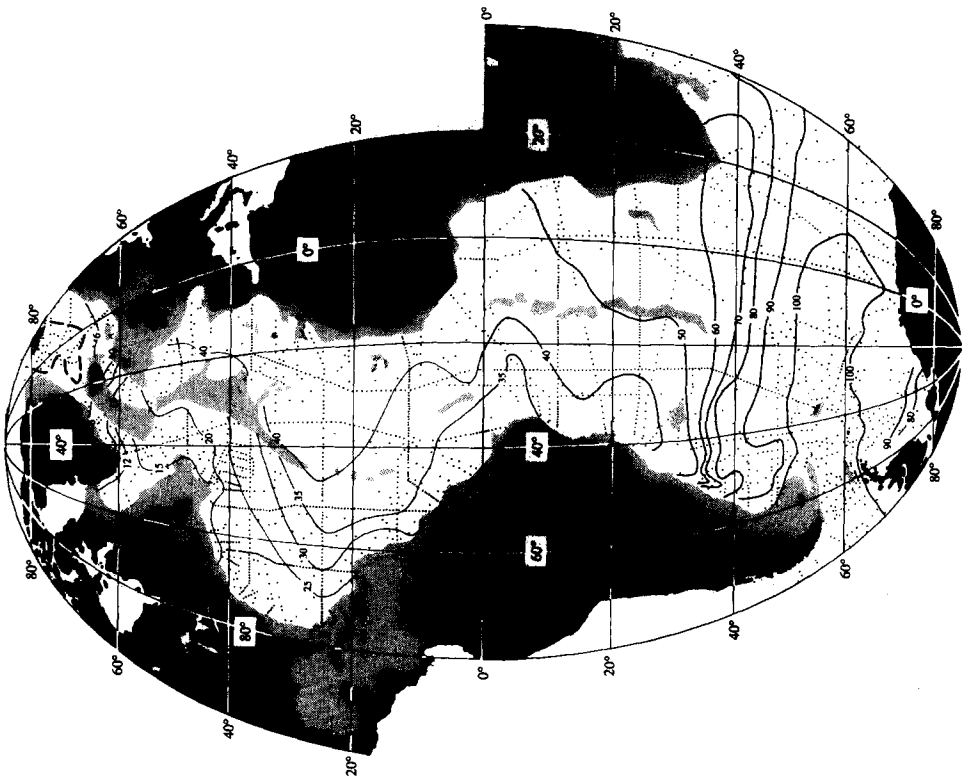

Fig. 16g. Silica (μm kg^{-1}) on the isopycnal defined by 41.50 in σ_3.

Fig. 17a, 17b

σ_4=45.88 Depth, S

Fig. 17a. Depth (hm) of the isopycnal defined by 45.88 in σ_4.

Fig. 17b. Salinity on the isopycnal defined by 45.88 in σ_4.

Fig. 17c, 17d
σ_4=45.88 O_2, NO_3

Fig. 17c. Oxygen (ml/l) on the isopycnal defined by 45.88 in σ_4.

Fig. 17d. Nitrate (μm kg^{-1}) on the isopycnal defined by 45.88 in σ_4.

Fig. 17e, 17f
σ_4=45.88 PO_4, SiO_3

Fig. 17e. Phosphate (μm kg^{-1}) on the isopycnal defined by 45.88 in σ_4.

Fig. 17f. Silica (μm kg^{-1}) on the isopycnal defined by 45.88 in σ_4.

Fig. 18a, 18b
σ_4=45.907 Depth, S

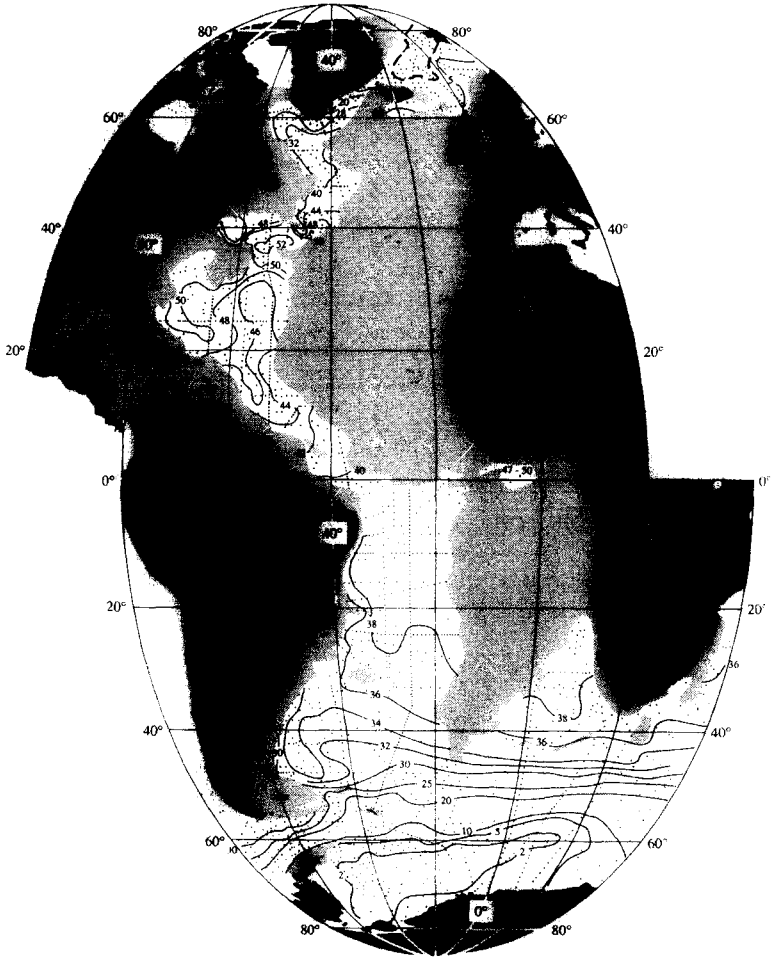

Fig. 18a. Depth (hm) of the isopycnal defined by 45.907 in σ_4.

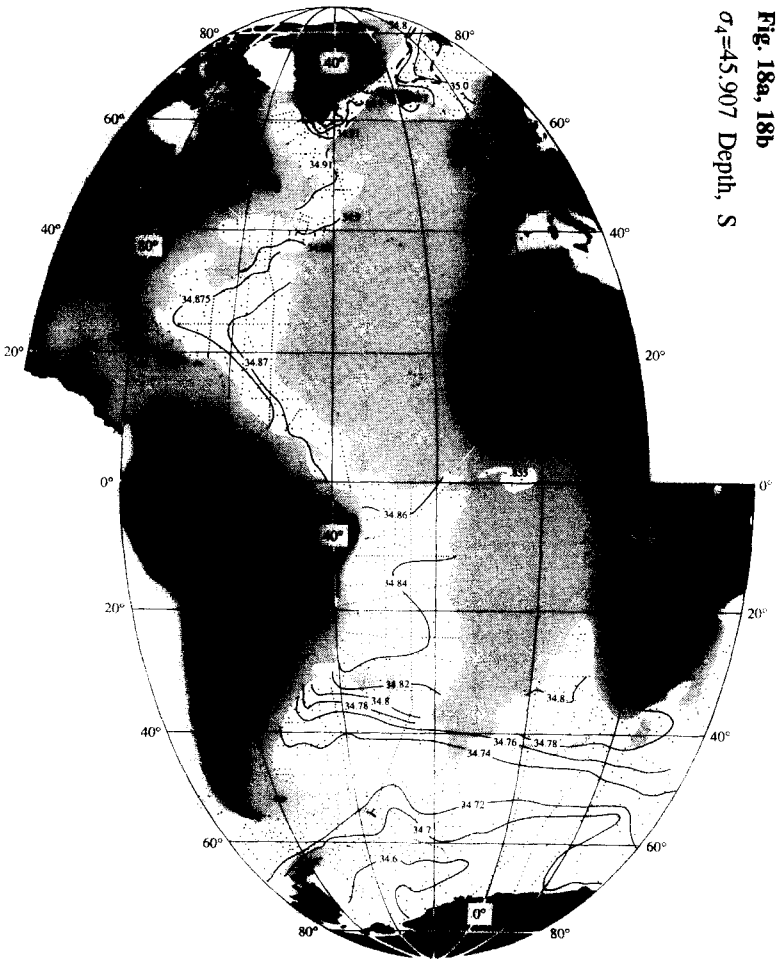

Fig. 18b. Salinity on the isopycnal defined by 45.907 in σ_4.

Fig. 18c
σ_4=45.907 O_2

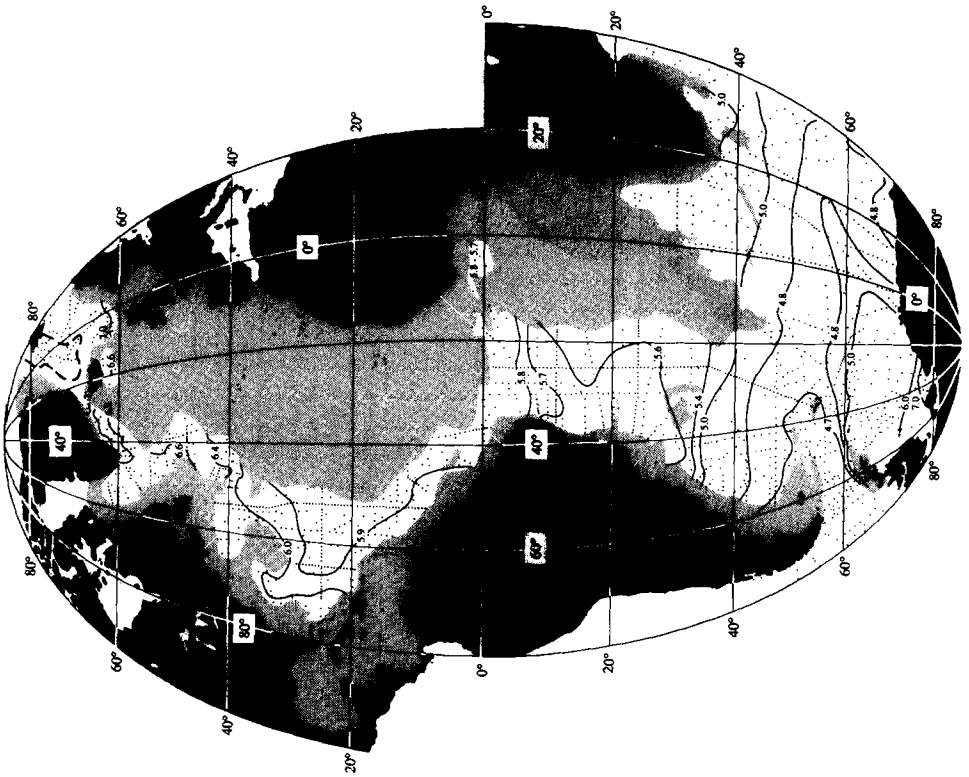

Fig. 18c. Oxygen (ml/l) on the isopycnal defined by 45.907 in σ_4.

Fig. 19a, 19b
σ_4=45.92 Depth, S

Fig. 19b. Salinity on the isopycnal defined by 45.92 in σ_4.

Fig. 19a. Depth (hm) of the isopycnal defined by 45.92 in σ_4.

Fig. 19c, 19d
σ_4=45.92 O_2, SiO_3

Fig. 19c. Oxygen (ml/l) on the isopycnal defined by 45.92 in σ_4.

Fig. 19d. Silica (μm kg^{-1}) on the isopycnal defined by 45.92 in σ_4.

Fig. 20
Bottom Θ

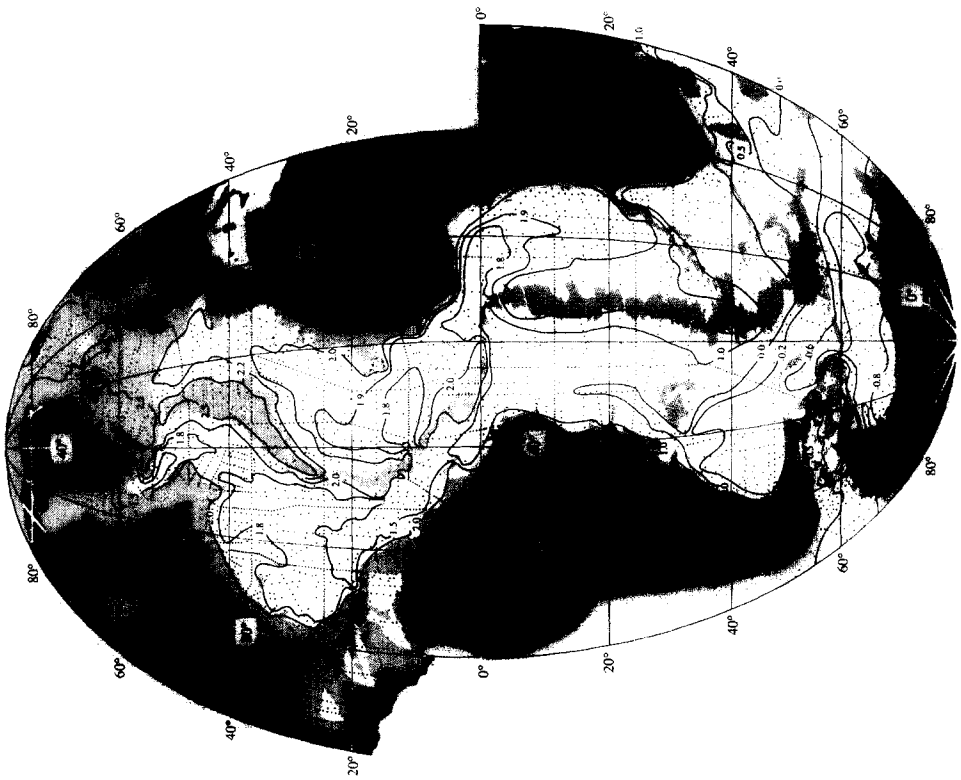

Fig. 20. Potential temperature (°C) at the bottom. Shaded areas represent depths less than 3500m. (Mantyla, work in progress).